

# Stability of the CMSSM against sfermion VEVs

---

J. E. Camargo-Molina<sup>a</sup> B. O’Leary<sup>a</sup> W. Porod<sup>a</sup> F. Staub<sup>b</sup>

<sup>a</sup>*Institut für Theoretische Physik und Astronomie, Universität Würzburg  
Am Hubland, 97074 Würzburg, Germany*

<sup>b</sup>*Bethe Center for Theoretical Physics & Physikalisches Institut der Universität Bonn,  
53115 Bonn, Germany*

*E-mail:* [jose.camargo@physik.uni-wuerzburg.de](mailto:jose.camargo@physik.uni-wuerzburg.de),  
[ben.oleary@physik.uni-wuerzburg.de](mailto:ben.oleary@physik.uni-wuerzburg.de), [porod@physik.uni-wuerzburg.de](mailto:porod@physik.uni-wuerzburg.de),  
[fnstaub@th.physik.uni-bonn.de](mailto:fnstaub@th.physik.uni-bonn.de)

**ABSTRACT:** The recent discovery of a Higgs boson by the LHC experiments has profound implications for supersymmetric models. In particular, in the context of restricted models, such as the supergravity-inspired constrained minimal supersymmetric standard model, one finds that preferred regions in parameter space have large soft supersymmetry-breaking trilinear couplings. This potentially gives rise to charge- and/or color-breaking minima besides those with the correct breaking of  $SU(2)_L \times U(1)_Y$ . We investigate the stability of parameter points in this model against tunneling to possible deeper color- and/or charge-breaking minima of the one-loop effective potential. We find that allowed regions of the parameter space with light staus or with light stops are seriously constrained by the requirement that there are no deeper minima, and the parameter space is still quite constrained even by the less strict requirement that the tunneling time out of the normal electroweak-symmetry-breaking vacuum is more than a fifth of the age of the known Universe. We also find that “thumb rule” conditions on Lagrangian parameters based on specific directions in the tree-level potential are of limited use.

**KEYWORDS:** supersymmetry, vacuum stability

---

## Contents

<b>1</b>	<b>Introduction</b>	<b>1</b>
<b>2</b>	<b>Analytical approximations for limits of charge- and color-breaking minima</b>	<b>4</b>
<b>3</b>	<b>Parameter point selection and stability evaluation</b>	<b>7</b>
3.1	Evaluating the SUSY-scale Lagrangian	7
3.2	Evaluating the stability of the effective potential	7
3.3	Dependence on which scalars are allowed non-zero VEVs	9
3.4	Robustness of numerical results	9
3.5	Scale and loop order dependence	11
3.6	Thermal effects	13
<b>4</b>	<b>Constraining relevant regions of the CMSSM parameter space</b>	<b>13</b>
4.1	Constraining $A_0$ and $\tan\beta$	13
4.2	Constraining the light stau parameter space	14
4.3	Constraining the light stop parameter space	19
4.4	Constraining the parameter space of $m_h \simeq 125$ GeV	20
<b>5</b>	<b>Discussion and conclusion</b>	<b>23</b>

---

## 1 Introduction

The standard model of particle physics (SM) [1–3] has proven itself to be an extremely good description of particle physics all the way up to the tera-electron-Volt scale. The interpretation of the bosonic resonance at 125 GeV recently discovered at the Large Hadron Collider (LHC) [4, 5] as the Higgs boson of the SM completes the picture, and allows us to probe the mechanism of the spontaneous breaking of gauge symmetries.

A particular issue, however, of the Higgs boson is that its mass, determining the electroweak scale, is many orders of magnitude smaller than the “natural” value of the order of the Planck scale. This, along with the fact that quantum corrections to the mass of the Higgs boson are typically of the scale of the heaviest particles which interact with it, leads to model builders attempting to resolve this “hierarchy problem”.

One popular way of ameliorating the hierarchy problem is to promote the SM to a supersymmetric theory, such as the minimal supersymmetric standard model (MSSM) (see [6] for a review). The MSSM contains all the particles and interactions of the SM as a subset, and the interactions of the supersymmetric partners are related to the SM interactions.

Usually one postulates a conserved parity known as  $R$ -parity [7] to avoid baryon- and lepton-number violating interactions which would be otherwise allowed by gauge symmetries and supersymmetry. The conservation of this parity, which we take here as part of the definition of the MSSM, implies the stability of the lightest supersymmetric partner (LSP), which, if uncharged under  $SU(3)_c \times U(1)_{EM}$ , is a candidate particle to explain the observed dark matter of the Universe.

In principle, the MSSM has *less* parameters than the SM, since the quartic coupling of the Higgs boson is actually a function of the gauge couplings. However, the mechanism of supersymmetry (SUSY) breaking must introduce more parameters, and agnosticism of the exact mechanism leads to the common practice of parametrizing the mechanism by adding *soft SUSY-breaking terms* to the Lagrangian density. The number of parameters specifying the full set of soft SUSY-breaking terms allowed in the MSSM is rather large, namely 105 [6], so often they are taken to be related at a specific scale. One of the simplest and most popular proposals is the minimal-supergravity-inspired constrained MSSM (CMSSM), in which all the soft SUSY-breaking scalar mass-squared terms are taken to be equal to  $M_0^2$  at the scale  $M_{GUT}$  where the gauge couplings unify, assuming that somehow the MSSM is a part of a grand unified theory (GUT). In addition, the soft SUSY-breaking mass terms for the fermionic partners of the gauge bosons are also taken to unify at  $M_{GUT}$  with a common value  $M_{1/2}$ . Finally a third GUT-scale common value is defined:  $A_0$ , a common trilinear scalar interaction coupling (multiplied by the corresponding Yukawa couplings). In principle, the  $\mu$  parameter coupling the Higgs doublets and the corresponding soft SUSY-breaking term  $B_\mu$  could also be defined at the GUT scale, but for practical reasons they are taken to be engineered by the requirement of correct electroweak symmetry breaking at a given scale, often the geometric mean of the masses of the two stops, the scalar partners of the top quark, referred to as the SUSY scale. The values of  $|\mu|$  and  $B_\mu$  are fixed by requiring that the mass of the  $Z$  boson is correct along with defining the ratio  $\tan\beta$  of the *vacuum expectation values* (VEVs)  $v_d$  and  $v_u$  of the neutral components of the two Higgs doublets, and the sign of  $\mu$  is given as a final input<sup>1</sup>.

The constraints of the CMSSM broadly lead to fixed ratios of the gaugino masses at the SUSY scale, and groupings of the squark masses together and the slepton masses together. The size of the gaugino masses and the masses of the groupings of sfermions relative to the gauginos are controlled by  $M_{1/2}$  and  $M_0$  respectively, and the only remaining freedom to change this spectrum lies in tuning  $A_0$  and  $\tan\beta$  to separate out the third-generation sfermions from the other generations.

The interplay between this handful of parameters is usually enough to explain many observations. For instance, requiring that the relic density of dark matter is within the uncertainties of the observed value might seem to significantly constrain the allowed parameter space [9]. However, if one fixes one or two of the CMSSM parameters, there is typically a range of the other parameters where the relic density is compatible with observations [10]. One particular region is known as the “stau co-annihilation region” [10], where the stau is marginally heavier than the lightest neutralino, which is the LSP, and freezes out only slightly earlier, allowing more annihilation before the neutralino freeze-out.

At the same time a mass of 125 GeV for the lightest MSSM Higgs boson is difficult to achieve without at least one stop with a multi-TeV mass [11–16]. One way to achieve this is to have a sufficiently high  $M_0$  so that the stop mass is large enough, and a sufficiently high  $M_{1/2}$  to bring the mass of the lightest neutralino up to just below the lightest stau mass (though for sufficiently high masses, the stau co-annihilation mechanism cannot reduce the relic density to the observed value, even for a vanishing mass difference between the stau and the lightest neutralino [10, 17]). However, this region of parameter space has rather bleak prospects for the discovery of sparticles. The only other way that this can be achieved within the CMSSM is through a large  $A_0$ , inducing a large splitting between the two mass eigenstates of both the staus and the stops. This allows the loop corrections to

---

<sup>1</sup>However, it has been noted in Ref. [8] that defining a Lagrangian partially at different scales is ambiguous and in the case of the CMSSM, different values of  $\mu$  and  $B_\mu$  at the GUT scale can lead to the same  $m_Z$  and  $\tan\beta$  at the SUSY scale while keeping  $M_0$ ,  $M_{1/2}$ , and  $A_0$  the same. This is indeed interesting, but beyond the scope of this work, where we identify CCB minima of SUSY-scale Lagrangians which were generated by CMSSM conditions.

the Higgs mass to be large through both the existence of a heavy stop and the large splitting between the stop mass eigenstates, while allowing at least some potentially LHC-accessible sparticles [18].

The presence of many additional scalar partners for the SM fermions raises the question of whether they too could develop VEVs. If, for example, the potential were such that stops would develop non-zero VEVs, then that would be disastrous as these VEVs would spontaneously break  $SU(3)_c$  and  $U(1)_{EM}$ ! Unfortunately until recently it was quite impractical to search for other vacua to see whether the desired vacuum is stable, or whether there are charge- and/or color-breaking (CCB) minima.

Since there are many different possibilities for vacua in the MSSM, spontaneously breaking any or all of the gauge symmetries, we denote the vacuum that should describe the Universe in which we live as the desired-symmetry-breaking (DSB) vacuum.

Some of the earliest work investigated the directions of the tree-level potential where the quartic terms vanish, as soft SUSY-breaking terms could lead to the potential being unbounded from below in these directions or to CCB minima deeper than the DSB vacuum developing along these directions [19–29]. Moreover, studies have been performed on the tunneling time between different vacua [30]. Certain conditions relating the trilinear parameters with the mass-squared parameters have been obtained which ensured that no deeper minimum could develop *along a line where the scalar fields have values in fixed ratios to each other*. However, it has been known for many years that it is only very special parameter points where this condition would be sufficient to forbid undesired minima, and that in general even at tree level it is very difficult to ensure that there are no undesired minima deeper than the desired minimum [31]. Moreover, despite various claims in the literature [28, 32], loop corrections are important: in [33], a numerical minimization of the one-loop effective potential including the top-quark Yukawa contributions has been performed demonstrating the importance of the corrections, and it was noted in [34] that loop corrections could change the ordering of which minimum is deepest.

It is possible that CCB minima could be tolerated [30, 35, 36], if the Universe would have fallen naturally into the false DSB vacuum as the cosmological temperature decreased, and if the lifetime of this vacuum for tunnelling into the true CCB vacuum is much longer than the present age of the Universe. Whether the DSB vacuum is in fact preferred by cosmology depends, in particular, on the scalar masses-squared generated during inflation. If these masses-squared are positive and of the order of the square of the Hubble parameter, the ‘more symmetric’ DSB vacuum is favored. On the other hand, if these are negative, the Universe would remain trapped in the true CCB vacuum [37]. A detailed discussion on these issues including the case of negative  $M_0^2$  at  $M_{GUT}$  and higher dimensional operators can be found in [38].

In the last few years there has been much progress in the field of determining the global minimum of the potential of a quantum field theory. In particular, the global minimum of renormalizable tree-level potentials (and other potentials of a purely polynomial form) can now be found deterministically with methods such as the Gröber basis method [39, 40] or the homotopy continuation method [41–43].

Recently the power of the homotopy continuation method for finding tree-level minima combined with gradient-based minimization with loop corrections has been combined in the publicly-available code **Vevacious** [44]. We use this tool to investigate regions of the CMSSM which, despite having local minima with the desired breaking of  $SU(2)_L \times U(1)_Y$  to  $U(1)_{EM}$  while preserving  $SU(3)_c$ , might have global minima with a different breaking of the gauge symmetries. This allows us to update existing studies [34, 45–47] by calculating *all* the tree-level extrema and the complete one-loop effective potential in the neighborhood of these extrema. This also allows us to check to what extent the existing rules are useful at all. This is particularly important in view of the fact that the explanation of the observed Higgs mass requires special parameter combinations.

This paper is organized as follows: in section 2 we collect the existing analytical approximations to determine color- and/or charge-breaking minima. In section 3, we briefly explain the tools that we used to generate the spectra of CMSSM points and to evaluate the stability of such points against undesired vacua. Then we consider how robust our results are against which scalars are allowed non-zero VEVs and against variations in scale, how dependent they are on loop corrections, and how the results might depend on the precise values of the Lagrangian parameters as evaluated by different spectrum generators; we also examine the usefulness of the tree-level conditions mentioned above. In section 4, we investigate part of the stau co-annihilation region to demonstrate that its parameter points generally are only metastable, and we also demonstrate that it is difficult to get light stops in the CMSSM without rapid tunneling to CCB vacua. In addition, we show the stability of regions compatible with the measured mass of the Higgs boson, and further demonstrate the irrelevance of the “thumb rules” to the parameter space regions of interest.

## 2 Analytical approximations for limits of charge- and color-breaking minima

The tree-level scalar potential,  $V^{\text{tree}}$  of the MSSM consists of three parts

$$V^{\text{tree}} = V_D + V_F + V_{\text{soft}} \quad (2.1)$$

with

$$V_D = \frac{1}{2} \sum_a g_a^2 \left( \sum_i \phi_i^\dagger T^a \phi_i \right)^2 \quad (2.2)$$

$$V_F = \sum_i \left| \frac{\partial W}{\partial \phi_i} \right|^2 \quad (2.3)$$

$$V_{\text{soft}} = \sum_i m_i^2 |\phi_i|^2 + (B_\mu H_d H_u + \text{H.c.}) + \sum_{\alpha=\text{generations}} \left( A_{u_\alpha} Y_{u_\alpha} H_u \tilde{Q}_\alpha \tilde{u}_{R,\alpha}^* + A_{d_\alpha} Y_{d_\alpha} \tilde{Q}_\alpha H_d \tilde{d}_{R,\alpha}^* + A_{l_\alpha} Y_{l_\alpha} \tilde{L}_\alpha H_d \tilde{e}_{R,\alpha}^* + \text{H.c.} \right) \quad (2.4)$$

where we have neglected flavor violation for simplicity. At the minimum the scalar fields take constant values. As a guide to aid in following the discussion on formulae based on  $V^{\text{tree}}$ , we show the case  $H_d = v_d/\sqrt{2}$ ,  $H_u = v_u/\sqrt{2}$ ,  $\tilde{\tau}_L = v_{L3}/\sqrt{2}$ ,  $\tilde{\tau}_R = v_{E3}/\sqrt{2}$ , all other scalars set to 0:

$$\begin{aligned} V_{H_d, H_u, \tilde{\tau}_L, \tilde{\tau}_R}^{\text{tree}} = & \frac{1}{32} (g_1^2 (v_d^2 - v_u^2 + v_{L3}^2 - 2v_{E3}^2)^2 + g_2^2 (v_d^2 - v_u^2 - v_{L3}^2)^2) \\ & + \frac{1}{4} Y_\tau^2 (v_d^2 v_{L3}^2 + v_d^2 v_{E3}^2 + v_{L3}^2 v_{E3}^2) + \frac{Y_\tau}{\sqrt{2}} v_{L3} v_{E3} (A_\tau v_d - \mu v_u) \\ & - B_\mu v_d v_u + \frac{1}{2} (|\mu|^2 (v_d^2 + v_u^2) + m_{H_d}^2 v_d^2 + m_{H_u}^2 v_u^2 + m_{\tilde{\tau}_L}^2 v_{L3}^2 + m_{\tilde{\tau}_R}^2 v_{E3}^2) \end{aligned} \quad (2.5)$$

The main focus of previous studies was to derive analytical conditions involving relevant parameters that would allow one to identify regions in parameter space without color- or charge-breaking minima. This led to a collection of “thumb rules” which do well only for specific extreme cases.

The most widespread of these is derived by making assumptions about the ratios of VEVs at CCB minima. Keeping the scalar fields at values in constant ratios to each other defines rays in field

configuration space. An example that we shall consider in a moment would be to take the stau fields to be equal to the down-type Higgs field:  $H_d = \tilde{\tau}_L = \tilde{\tau}_R$ , and all other fields held to zero. Along such rays, the potential can be written as a function of a single variable, such as the normalized magnitude of the VEVs. The key observation underpinning the widespread thumb rules is that the  $D$ -term contributions to the potential vanish along certain rays, removing their “stabilizing” influence (as they are always positive for non-zero values of the scalar fields). Hence one might suspect that undesired minima would lie in such regions; so that along these rays, one can solve the one-dimensional minimization condition (the  $F$ -terms ensure that the potential is still bounded from below), and compare the minimum along this ray to the DSB minimum.

Along a ray where the  $D$ -terms vanish, one can cast the tree-level potential in the form

$$V^{\text{tree}} = \frac{m^2}{2}v^2 - \frac{YA}{3}v^3 + \frac{Y^2}{4}v^4 \quad (2.6)$$

where  $v$  is the (scaled) length of the vector of field values. This is minimized when

$$v = \frac{A + \sqrt{A^2 - 4m^2}}{2Y} \quad (2.7)$$

(or when  $v = 0$ , where the tree-level potential is zero). Since the desired normal EWSB vacuum has a negative value for the tree-level potential, it is then sufficient to ensure that the potential along this ray is never negative. Plugging the above value of  $v$  into  $V^{\text{tree}}$  and demanding that the potential is positive independent of the sign of  $A$  shows that the dependence on  $Y$  is just an overall factor, and that the potential is positive at this field configuration regardless of the value of  $Y$  as long as the condition

$$m^2 > \frac{2}{9}A^2 \quad (2.8)$$

is satisfied, which then unpacks into various conditions, depending on which rays are taken.

One of the simplest rays along which the  $D$ -terms of eq. (2.5) vanish is the direction where  $H_u$  is taken to be 0, and  $H_d = \tilde{\tau}_L = \tilde{\tau}_R = 3^{-1/4}v$ , where the factor of  $3^{-1/4}$  keeps the quartic term correctly normalized when casting the potential in the form of eq. (2.6) and thus  $m^2 = (m_{H_d}^2 + |\mu|^2 + m_{\tilde{\tau}_L}^2 + m_{\tilde{\tau}_R}^2)/\sqrt{3}$  and  $A = 2^{-1/2}3^{1/4}A_\tau$ . This leads to a widely-used condition [19–23]

$$A_\tau^2 < 3(m_{H_d}^2 + |\mu|^2 + m_{\tilde{\tau}_L}^2 + m_{\tilde{\tau}_R}^2) \quad (2.9)$$

and the analogous condition for stop VEVs is

$$A_t^2 < 3(m_{H_u}^2 + |\mu|^2 + m_{\tilde{t}_L}^2 + m_{\tilde{t}_R}^2). \quad (2.10)$$

In Ref. [28] an improved set of conditions were given, which for example for the first generation take a similar form as above, e.g.

$$A_u^2 < 3(m_{H_u}^2 + m_{\tilde{u}_L}^2 + m_{\tilde{u}_R}^2). \quad (2.11)$$

As here no large Yukawa couplings are involved, this can readily be expressed using the high scale parameters of the CMSSM [48]

$$(A_0 - 0.5M_{1/2})^2 < 9M_0^2 + 2.67M_{1/2}^2 \quad (2.12)$$

This condition was derived explicitly for the VEVs of the sfermions of the first two generations as it relies on the Yukawa couplings being much smaller than the gauge couplings. This is manifestly not

the case for the stop sector, nor for the stau sector for parameter points with large  $\tan\beta$ , and was noted as such. However, it is worth examining how well such conditions do for the third generation nevertheless, given the lack of any other simple expressions for stop or stau VEVs. Henceforth when we refer to condition (2.11), we take the parameters for the *third* generation of up-squark, i.e. the stop, as opposed to the first generation:  $A_t^2 < 3(m_{H_u}^2 + m_{\tilde{t}_L}^2 + m_{\tilde{t}_R}^2)$ .

Since we will be plotting the lines between points which satisfy these conditions quite frequently, we note here the color scheme that we use. The solid colored lines correspond to the dividing lines between parameter points that satisfy or fail the conditions as following: condition (2.9) by purple, condition (2.10) by orange, condition (2.11) by dark red, and condition (2.12) by brown. We do not plot any of these lines in white regions in our figures, where no spectra could be calculated for the DSB minimum anyway, due to the presence of tachyons.

For the third generation, the expressions are considerably more complicated, and a numerical approach is usually necessary to get reasonable results. An algorithm to extract CCB minima of the tree-level potential assuming vanishing (color)  $D$ -terms and either stau or stop VEVs (but not both at once) was presented in Ref. [28]. The authors assumed that  $\tan\beta = \frac{v_u}{v_d} > 1$  holds even at the CCB minimum, while our ansatz is more general and we find that often  $\tan\beta < 1$  holds at the global minimum for points with stop VEVs. We will also later compare our numerical results with the analytical constraints summarized above.

Another algorithm was presented in [49] for the limiting case of  $\tan\beta \rightarrow \infty$ . The algorithm only goes so far as to give a very conservative upper bound on  $|A_t|$  to ensure that there is no minimum of the tree-level potential when the only non-zero VEVs are those for  $H_u$ ,  $\tilde{t}_L$ , and  $\tilde{t}_R$ . Since, as will be seen, the limit of large  $\tan\beta$  is characterized by *stau* VEVs rather than stop VEVs within the CMSSM, the condition is not very helpful, as will be shown. Rather than implement the full numerical algorithm, however, we plot lines dividing points which fail

$$A_t^2 < (0.65 - 0.85)^2(3(m_{\tilde{t}_1}^2 + m_{\tilde{t}_2}^2 + 2m_t^2)) \quad (2.13)$$

from those which pass in dark blue, where we have chosen 0.65 from the point where the CCB condition diverges from the tachyonic stop line in figure 1 of [49] to 0.85 as being close to the maximal allowed value from the optimal bound therein.

It has already been reported in the literature that these conditions are neither necessary nor sufficient to ensure that the desired minimum is the global minimum, even at tree level [25, 34]. Note that the condition (2.8) is *sufficient* to guarantee that *along this ray*, there is not a deeper undesired minimum, but not *necessary*. However ensuring that there is no deeper minimum along this ray is *necessary* but *not sufficient* to guarantee that there is no deeper minimum than the DSB minimum. The interplay of this logic is though that this condition is *neither necessary nor sufficient* to ensure that there is not a deeper undesired minimum for a field configuration which does not lie on this ray. There could be an undesired minimum along this ray that has a negative tree-level potential value, yet is not as negative as that of the DSB vacuum, or there could be a deeper undesired minimum which does not lie on the ray even though there is no point on the ray itself that has a negative tree-level potential energy.

Recently, the hints for an enhanced di-photon decay rate have revived the interest in charge-breaking minima since the only possibility to explain this enhancement in the MSSM which does not affect the other decay channels would be very light staus [50, 51]. In this context, new checks for



charge-breaking minima due to stau VEVs have been derived or revived [52, 53]:

$$\mu \tan \beta < 213.5 \sqrt{m_{\tilde{\tau}_L} m_{\tilde{\tau}_R}} - 17.0(m_{\tilde{\tau}_L} + m_{\tilde{\tau}_R}) + 4.52 \times 10^{-2} \text{ GeV}^{-1} (m_{\tilde{\tau}_L} - m_{\tilde{\tau}_R})^2 - 1.30 \times 10^4 \text{ GeV} \quad (2.14)$$

$$|(Y_\tau v_u \mu)/(\sqrt{2} m_\tau)| < 56.9 \sqrt{m_{\tilde{\tau}_L} m_{\tilde{\tau}_R}} + 57.1(m_{\tilde{\tau}_L} + 1.03 m_{\tilde{\tau}_R}) - 1.28 \times 10^4 \text{ GeV} + \frac{1.67 \times 10^6 \text{ GeV}^2}{m_{\tilde{\tau}_L} + m_{\tilde{\tau}_R}} - 6.41 \times 10^6 \text{ GeV}^3 \left( \frac{1}{m_{\tilde{\tau}_L}^2} + \frac{0.983}{m_{\tilde{\tau}_R}^2} \right) \quad (2.15)$$

where  $m_\tau$  is the pole mass of the fermionic  $\tau$  lepton. The condition given by (2.14) was obtained by a numerical fit of the result of a scan to an ansatz in Ref. [52]. Likewise, condition (2.15) also comes from a fit of the results of a scan to an ansatz in Ref. [53]. The form of the condition which we present here comes from combining the definition of  $\tan \beta_{\text{eff}}$  from eq. (4) in Ref. [53] with their condition (10).

We also mention here that the dividing line between passing and failing condition (2.14) is plotted in pink in the following figures, and condition (2.15) in grey. Again, if these lines would only appear in white regions of our figures, we do not plot them.

Note that conditions (2.14) and (2.15) were obtained assuming that  $A_\tau = 0$ . Thus in the context of the CMSSM, where one needs large, negative  $A_0$  to explain the Higgs mass by the stop loops, it can already be expected that these limits will not be very helpful.

We are going to discuss CMSSM scenarios where light staus and stops appear and point out that these scenarios are often ruled out by an unstable DSB vacuum which is not indicated by any of the above thumb rules.

### 3 Parameter point selection and stability evaluation

#### 3.1 Evaluating the SUSY-scale Lagrangian

Since parameter points of the CMSSM are defined by mixtures of GUT- and SUSY-scale parameters, it is impossible to investigate a parameter point without having calculated the full renormalization group running of the full Lagrangian from one scale to the other. Several programs are available for public use that do this job: **ISAJET** [54, 55], **SoftSUSY** [56], **SPheno** [57, 58], or **SuSpect** [59], for example. All of these codes have been shown to agree quite well [60]. We chose to evaluate all our points with a **SPheno** module created by **SARAH** [61–64] and show a comparison to **SoftSUSY** in section 3.4.

On a technical level, the input flags were set such that the renormalization group equations (RGEs) were evaluated with two-loop beta functions. The following values were used for the SM parameters:

$$\alpha^{-1}(M_Z) = 127.93, \quad G_F = 1.166370 \cdot 10^{-5} \text{ GeV}^{-2}, \quad \alpha_S = 0.1187, \quad m_Z = 91.1887 \text{ GeV}, \\ m_b(m_b) = 4.18 \text{ GeV}, \quad m_t = 173.5 \text{ GeV}, \quad m_\tau = 1.7769 \text{ GeV} \quad (3.1)$$

The entire mass spectrum was evaluated at one loop, i.e. the known two-loop corrections [65–69] were neglected, in order to have a consistent input to evaluate the one-loop effective potential without having to worry about whether higher orders may affect the consistency of the calculation.

#### 3.2 Evaluating the stability of the effective potential

The purpose of this work is to determine how stable the DSB local minimum of the MSSM potential is against possible deeper minima with different patterns of broken symmetries. Throughout our investigation we use **Vevacious** (version 1.0.11) to determine the stability of CMSSM parameter



points. We use the full one-loop effective potential, and we refer the reader to the **Vevacious** manual [44] for details.

We use the MSSM model files provided by default, which were generated with **SARAH** 4 [70]. Unless otherwise stated, we allow six scalar fields to obtain non-zero VEVs, which are assumed to be real: the neutral components of the two Higgs doublets  $H_d$  and  $H_u$  (with VEVs  $v_d$  and  $v_u$  respectively), “left-handed” stau  $\tilde{\tau}_L$  (with VEV  $v_{L3}$ ), “right-handed” stau  $\tilde{\tau}_R$  (with VEV  $v_{E3}$ ), and one color of “left-handed” and “right-handed” stops  $\tilde{t}_L$  and  $\tilde{t}_R$  (with VEVs  $v_{Q3}$  and  $v_{U3}$  respectively).

There is a certain amount of arbitrariness in deciding how long a tunneling time from the DSB vacuum to a different vacuum is acceptable. We chose to distinguish between parameter points where the tunneling time out of the DSB vacuum is greater than or less than 0.217 times the age of the known Universe (which we take to be 13.8 billion years), i.e. three billion years. We denote metastable parameter points with tunneling times less than three gigayears as *short-lived* and those with longer tunneling times as *long-lived*. A naïve estimate then of the DSB false vacuum surviving the observed 13.8 gigayears with a tunneling time of three gigayears, assuming a Poisson distribution, is one percent. The default threshold used by **Vevacious** if not overridden is 1.38 billion years (i.e. a tenth of the age of the known Universe), but since the tunneling time drops very rapidly (exponentially in the bounce action), the shift in the dividing line between a tunneling time of 1.38 gigayears and three gigayears is not even visible on our plots.

In addition, we note that the tunneling time calculation depends on numerical routines that try to find the optimal tunneling path between the DSB and CCB minima which minimizes the bounce action. It might happen sometimes that **CosmoTransitions** fails to find the optimal tunneling path and short-lived minima get labeled as long-lived. This manifests as apparently ragged borders between areas of short- and long-lived metastable points, and occasional islands of long-lived parameter points appearing in predominantly short-lived parameter point regions. To be conservative, we chose to keep the long-lived label for such points although we are quite certain that they are short-lived.

We note that there is a slight inconsistency in allowing CMSSM parameter points with flavor violation occurring in the Lagrangian and using model files allowing for only one generation of sfermions to have non-zero VEVs, as the tadpole equations for VEVs for the other two generations will not be satisfied in general for non-zero VEVs for both Higgs and third-generation sfermions. However, since the off-diagonal elements of the Yukawa matrices and trilinear soft SUSY-breaking terms are in general very small, the induced VEVs would be also in general very small, and evaluating the stability of the DSB minimum with respect to tunneling to a field configuration very close to the proper three-generation minimum should be sufficient. We note that this approximation (that small VEVs for first and second generation sfermions are neglected) certainly cannot produce an incorrect diagnosis of a parameter point as being metastable, as a three-generation minimum cannot be less deep than the nearby field configuration with zero VEVs for the first and second generation sfermions.

The applied procedure is quite conservative and we want to emphasize that any parameter points that we find to be metastable are definitely not absolutely stable, as we have found at least one counterexample minimum to the statement “this parameter point does not have any deeper minima than the DSB minimum” regardless of whether there are even deeper minima that we have not found (either because of the slight increase in depth by allowing more generations to have non-zero VEVs or because there are deeper minima that develop at the one-loop level that are not found by the **Vevacious** algorithm). Conversely, we do not claim that parameter points that we label as stable are guaranteed to be stable: we merely use it as a shorthand for the statement that we did not find any deeper minima and so to the best of our knowledge, the parameter point has a stable DSB minimum. Likewise, points found to be long-lived possibly might be short-lived, but short-lived points definitely

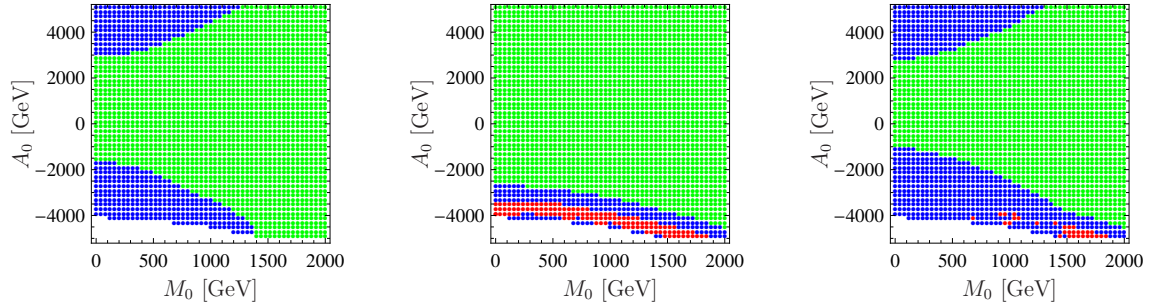


**Figure 1.** Vacuum stability in the  $(M_0, A_0)$ -plane for input values of  $\tan\beta = 10$ ,  $M_{1/2} = 1$  TeV and  $\mu > 0$ . (Here and in the other figures,  $\tan\beta$  is taken to mean the input parameter for the DSB vacuum.) On the left, we allow only for stau VEVs, in the middle only for stop VEVs and on the right for both stau and stop VEVs. Green indicates that no CCB minimum deeper than the DSB minimum was found, while blue and red indicate that the DSB minimum is only metastable, as there is at least one deeper CCB minimum. The red points are short-lived, while the blue points are long-lived, compared to a threshold of three gigayears. The lack of a smooth boundary between red and blue is a numerical artifact and is discussed in the text.

are short-lived, as any deeper minima will not make the DSB minimum more stable against tunneling to the CCB minimum that we found.

The MSSM model files were validated as reproducing the correct one-loop tadpole equations in the vicinity of the DSB minimum, as well as the correct tree-level running masses, which are the important part of the one-loop corrections. Furthermore, the case of allowing stau VEVs (but not stop VEVs) agrees with the expressions of Ref. [34], noting the different sign convention for the Yukawa terms.

### 3.3 Dependence on which scalars are allowed non-zero VEVs

Most checks in literature for CCB minima, which we are going to discuss in more detail in the following, assume that there are either stau or stop VEVs, but not both non-zero at the same time. However, we point out that it is not necessarily possible to treat them separately. In figure 1 we show the long- and short-lived points in the  $(M_0, A_0)$  plane allowing either only stau or only stop or stau and stop VEVs. One can see that the trivial overlaying of the two special cases does not reproduce the more general case. The entire range of  $A_0$  between -2 and +3 TeV seems to have a stable vacuum if one studies only stau or stop VEVs. However, allowing for both VEVs one can see that the vacuum is just metastable for  $A_0 < -1.5$  TeV and small values of  $M_0$ . Therefore in the CMSSM it is especially necessary for intermediate values of  $\tan\beta$  to check carefully for all possible combinations for stau and stop VEVs. Just in the limit of large or small  $\tan\beta$  checks for pure stau respectively stop VEV scenarios might be sufficient.

### 3.4 Robustness of numerical results

One might worry about how sensitive the presence of CCB minima is to the exact values used, and whether the small (understood) differences between values of parameters in different renormalization schemes could change the conclusion as to whether a parameter point is stable or metastable.

In lieu of an exhaustive duplication of plots, we compare the results along a line in the CMSSM parameter space using two different MSSM spectrum generators, with two different renormalization schemes: **SPheno** and **SoftSUSY**. Both are known to agree well on the physical observables, but the

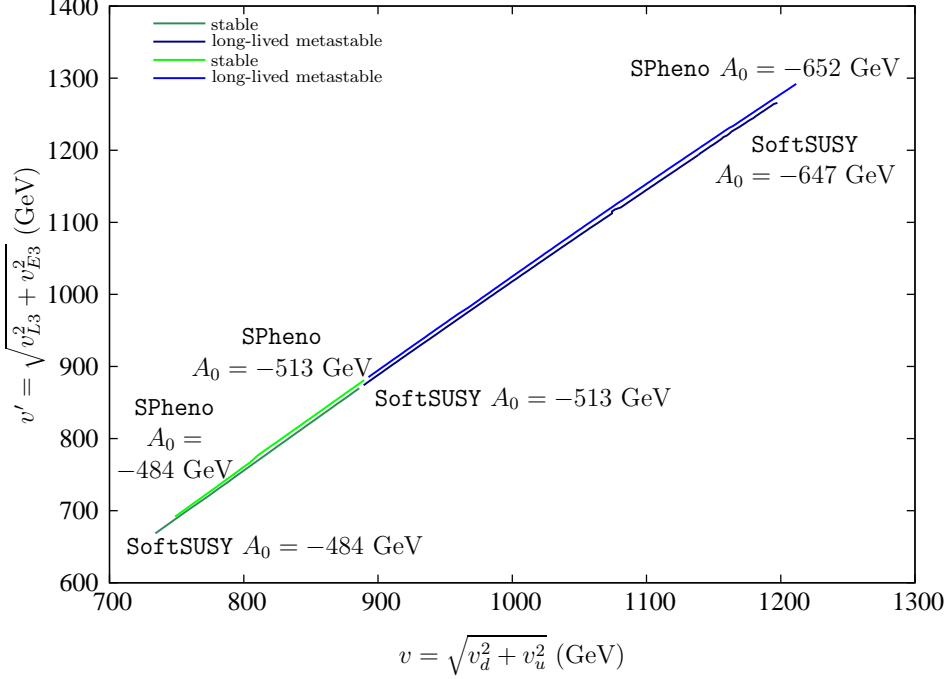


**Figure 2.** Comparison of the evolution of a charge-breaking minimum evaluated with **SPheno** and with **SoftSUSY**, starting from SPS4 and decreasing  $A_0$ , as a trajectory in Higgs VEV vector length  $v$  and stau VEV vector length  $v'$ . Similarly to as in figure 1, the green segment denotes parameter points where the DSB vacuum is stable, and the blue where it is long-lived metastable. Both sets of line segments are very close together. The line evaluated with **SoftSUSY** has darker shades for its segments than the line evaluated with **SPheno** has.

Lagrangian parameters differ, as **SoftSUSY** uses the modified  $\overline{\text{DR}}$  scheme described in [71] while we use **SPheno** in a scheme where the values of  $v_d$  and  $v_u$  at the DSB minimum do not change with loop corrections, as described in the appendix of [72].

The line that we choose is that which is obtained by starting at SPS4 [73] and decreasing  $A_0$  from zero to the point where the lightest neutralino is no longer the lightest supersymmetric partner. This entire line has been ruled out by the LHC already, as the masses of the colored sparticles are too light all along it, but it serves as an example.

In figure 3.4, we show a projection of the co-ordinates of the DSB minimum of SPS4 and the first other minimum of the potential (excluding minima related to the input minimum by gauge transformations) that develops, in the plane of the length  $v = \sqrt{v_d^2 + v_u^2}$  of the Higgs VEVs and the length  $v' = \sqrt{v_{L3}^2 + v_{E3}^2}$  of the stau VEVs. (As in section 2, the VEV of  $\tilde{\tau}_L$  is given by  $v_{L3}/\sqrt{2}$  and that of  $\tilde{\tau}_R$  by  $v_{E3}/\sqrt{2}$ .) The inputs of SPS4 ( $M_0 = 400$  GeV,  $M_{1/2} = 300$  GeV,  $\tan\beta = 50$ ,  $|\mu| > 0$ ) were held constant while  $A_0$  was varied from 0 GeV (the input for SPS4) to the value where even the DSB minimum is phenomenologically uninteresting as the stau is the LSP ( $-652$  GeV according to **SPheno**,  $-647$  GeV according to **SoftSUSY**). The input parameters were run with **SPheno** and with **SoftSUSY** from the GUT scale to the SUSY scale  $\sqrt{m_{\tilde{t}_1} m_{\tilde{t}_2}}$ .

The CCB minimum that develops along this line in parameter space only comes into existence once  $|A_0|$  gets large enough, and as  $|A_0|$  increases, it becomes deeper and eventually becomes deeper

$A_0$	generator	$v_d$	$v_u$	$v_{L3}$	$v_{E3}$
-484	<b>SPheno</b>	184	726	409	558
-484	<b>SoftSUSY</b>	181	712	394	540
-513	<b>SPheno</b>	269	851	540	701
-513	<b>SoftSUSY</b>	274	846	532	694
-652	<b>SPheno</b>	485	1110	819	999
-647	<b>SoftSUSY</b>	481	1097	800	981

**Table 1.** Full VEV configurations of the CCB minimum that develops by changing the input of SPS4 by making  $A_0$  negative, for endpoints of the segments of figure 3.4, where all dimensionful quantities are to be understood as in units of GeV.

than the DSB minimum, as one might have expected. Both **SPheno** and **SoftSUSY** agreed that the CCB minimum developed at  $A_0 = -431$  GeV and that it became deeper than the DSB minimum at  $A_0 = -513$  GeV. The details of the tunneling time for larger values of  $|A_0|$  did not match exactly but were nevertheless acceptably close, given that the tunneling time varies exponentially in the bounce action.

Both generators also yielded values for the VEVs at the CCB minima that agreed within the ranges expected for the differences between the programs, as can be seen in figure 3.4 and in table 1. Furthermore, as one can see in table 1, the values of the VEVs at the CCB minimum do not vary wildly as  $A_0$  is varied, and they remain quite safely within a few times the renormalization scale; hence the loop expansion should be trustworthy. For completeness, we note that, as expected, the VEVs increase for larger  $|A_0|$  and appear to be tending towards ratios that minimize the  $D$ -term contribution to the effective potential. Furthermore, one can clearly see how much the ratios of  $v_d$ ,  $v_{L3}$ , and  $v_{E3}$  at the global minima deviate from the ratio 1:1:1 that is assumed in the derivation of condition (2.9). Finally, we note in passing that conditions (2.9) – (2.15) are all satisfied along the entire line in parameter space from  $A_0 = 0$  GeV to  $A_0 = -652$  GeV.

### 3.5 Scale and loop order dependence

It is well known that parameters like masses or cross-sections suffer usually from a sizable scale dependence when they are calculated just at tree level. To reduce this dependence on the renormalization scale  $Q$ , higher-order corrections have to be taken into account. In the MSSM, the geometric average  $\sqrt{m_{\tilde{t}_1} m_{\tilde{t}_2}}$  of the stop masses is usually taken as renormalization scale, since it is expected that the  $Q$  dependence of the Higgs mass is minimized around this scale. A similar statement can be made about the vacuum stability: if one just considers the tree-level potential, the areas with CCB minima can be significantly shifted by changing the renormalization scale. This is shown in the left column of figure 3, where we show the results for  $Q = \sqrt{m_{\tilde{t}_1} m_{\tilde{t}_2}}/2$ ,  $Q = \sqrt{m_{\tilde{t}_1} m_{\tilde{t}_2}}$ , and  $Q = 2\sqrt{m_{\tilde{t}_1} m_{\tilde{t}_2}}$ . However, if one goes to the full one-loop effective potential, the sensitivity on the scale is significantly reduced, as depicted in the right column of figure 3. For completeness we note that that even for  $A_0 = 0$  one still has sizable  $A$ -parameters proportional to  $-M_{1/2}$  at the electroweak scale which cause the instability of the potential for small  $M_0$ .

We also note that this is an explicit example that undermines arguments that radiative effects do not change tree-level conclusions on the absolute stability of vacua such as in [32], as it is plain to see that even relatively small changes of scale can radically change tree-level conclusions.

The interesting possibility of bound states composed of stops has been suggested in the literature for extremely large  $|A_t|$  [74] and the effective Lagrangian in terms of these bound states could have

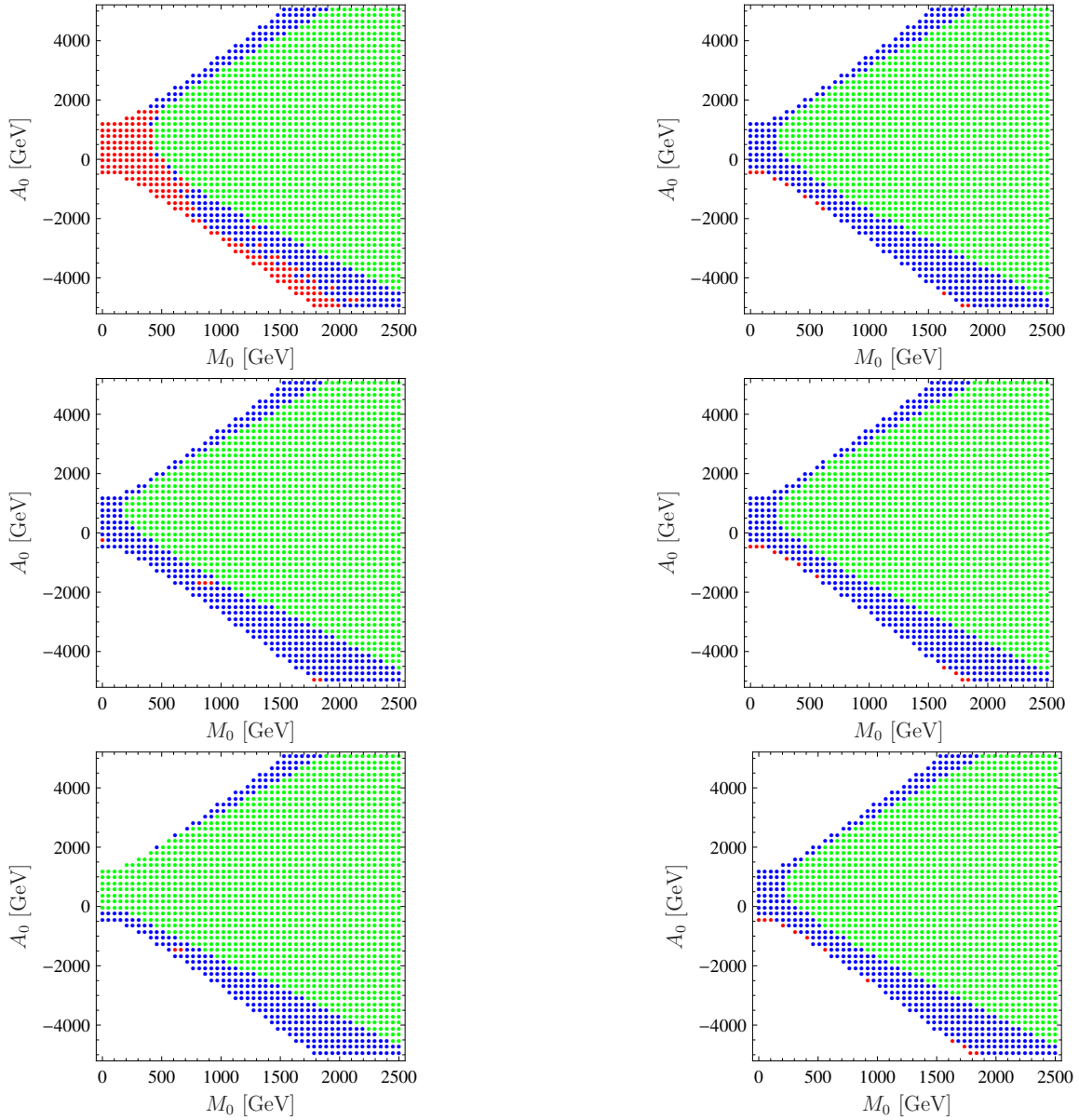


**Figure 3.** Vacuum stability in the  $(M_0, A_0)$  plane for fixed  $M_{1/2} = 1$  TeV,  $\mu > 0$  and  $\tan \beta = 40$ . On the left, only the tree-level potential was considered. On the right, the full one-loop effective potential was taken into account. The renormalization scale was  $Q = \sqrt{m_{\tilde{t}_1} m_{\tilde{t}_2}}/2$  (first row),  $Q = \sqrt{m_{\tilde{t}_1} m_{\tilde{t}_2}}$  (second row), and  $Q = 2\sqrt{m_{\tilde{t}_1} m_{\tilde{t}_2}}$  (last row). The color code is the same as in figure 1.

yet more minima which could be deeper than the DSB minimum. However, such a mechanism is very non-perturbative and does not look possible within the CMSSM, at least in the parameter regions which we investigate in this paper, and also certainly the existence of extra minima to which the DSB false vacuum can tunnel cannot *reduce* the decay width hence cannot increase the tunneling time.

### 3.6 Thermal effects

Of course, even if a parameter point has an acceptably long tunneling time out of the DSB vacuum at zero temperature, it may be the case that the false vacuum would not survive a period at a sufficiently high temperature below the critical temperature where the undesired minimum becomes less deep. While the one-loop thermal corrections are known [75] and implemented in `CosmoTransitions` [76], the evaluation of the minimal bounce action at non-zero temperature is currently unfeasibly slow for our work, and conclusions on the stability of a parameter point are strongly dependent on the assumed thermal history of the Universe. Hence we postpone such an investigation for future work.

## 4 Constraining relevant regions of the CMSSM parameter space

### 4.1 Constraining $A_0$ and $\tan\beta$

We start with a check for regions in the CMSSM space which don't have any CCB vacuum deeper than the DSB minimum. This gives us already some hint as to which regions of the parameter space are 'safe', and also where one has to perform more dedicated checks, as discussed in the following. For this purpose we look for the maximal value of  $|A_0|$  allowed for a given combination of  $M_0$ ,  $M_{1/2}$ ,  $\tan\beta$  and  $\text{sign}(\mu)$ , assuming that  $A_0 < 0$ . We concentrate on negative  $A_0$  as it has some preference due to the Higgs mass measurements [77]. The result is shown in figure 4. Note that this also restricts the smallest mass allowed for the lighter stau and stop, as discussed in sections 4.2 and 4.3. We see that the maximal value of  $|A_0|$  allowed is rather restricted, especially for large  $\tan\beta$ . The main reason is that the larger  $\tan\beta$  gets, the smaller  $m_{\tau_R}^2$  gets while keeping all other parameters fixed. That the electroweak minimum is destabilized for large  $\tan\beta$  is a feature which we are going to see often in the following.

As a next step, we investigate the problem of deeper minima further and check not only if there are deeper vacua but also if the DSB vacuum would be long- or short-lived. As mentioned in section 3.2, we take a relatively conservative threshold of 0.217 times the observed life time of the known Universe (corresponding to a one per-cent survival probability) to categorize metastable points as long-lived or short-lived. We present the distribution of stable, long- and short-lived vacua according to this definition in the  $(\tan\beta, A_0)$  plane for fixed values of  $M_0 = M_{1/2} = 1$  TeV and  $\mu > 0$  in figure 5. We show also a comparison with the regions excluded by the limits using the conditions (2.12) to (2.15). One can see that at least some analytical limits produce the qualitative dependence on  $\tan\beta$  but not one of them is really accurate and they miss many short-lived vacua. Note that those limits do not distinguish between long- and short-lived vacua but only assess the presence of a deeper CCB vacuum. Hence one has to compare them with the division between the stable (green) areas and the metastable (blue and red) areas, rather than how well they would separate long-lived (blue) from short-lived (red). It is then clear that even a combination of all of those rules would not exclude about half the points of our scans with CCB vacua deeper than the DSB vacua.

We note that the values of  $M_{1/2}$  and  $M_0$  of 1 TeV are rather close to those of the central values of CMSSM best-fit point after including a mass for the Higgs boson of 126 GeV of [18] ( $M_{1/2} = 1167.4_{-513.0}^{+594.0}$  GeV,  $M_0 = 1163.2_{-985.7}^{+1185.3}$  GeV,  $\tan\beta = 39.3_{-32.7}^{+16.7}$ ,  $A_0 = -2969.1_{-1234.9}^{+6297.8}$ ), and that the central values for  $\tan\beta$  and  $A_0$  are within the long-lived metastable region of figure 5. This seems to be rather endemic to models where the stau mass and the stop mass are related, for trying to fit both the dark matter relic abundance, requiring light staus, and a relatively heavy Higgs boson, requiring heavy stops, thus pushing the fit to large trilinear terms in the CMSSM. It also occurs regardless of allowing non-universal Higgs masses: the central values of the NUHM1 "low" best-fit point of [78] also

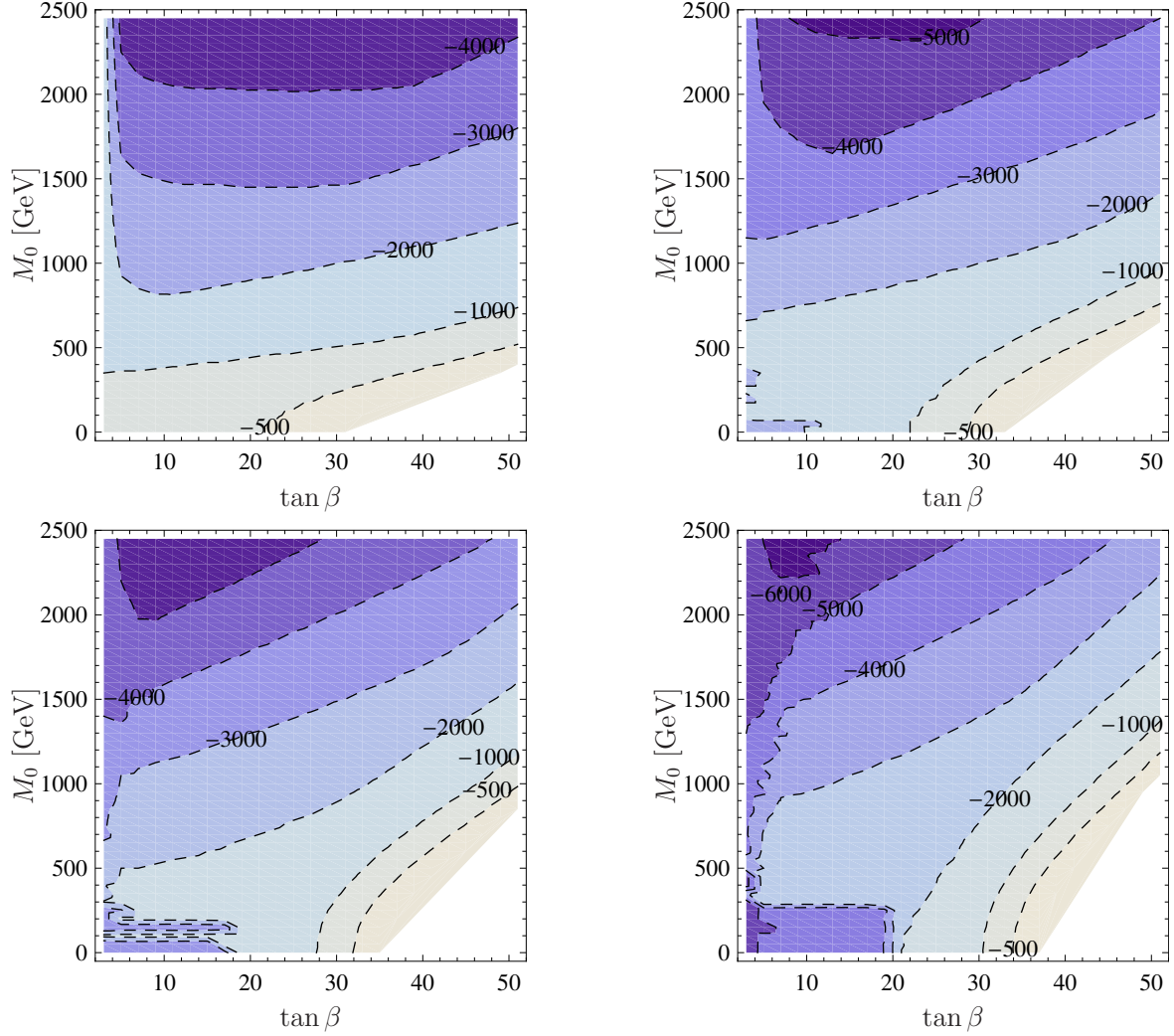


**Figure 4.** Minimal value allowed for  $A_0$  in the  $(\tan\beta, M_0)$  plane to have a stable DSB vacuum. We used  $\mu > 0$  and  $M_{1/2} = 500$  GeV (upper left),  $M_{1/2} = 1000$  GeV (upper right),  $M_{1/2} = 1500$  GeV (lower left) and  $M_{1/2} = 2000$  GeV (lower right).

result in a CCB global vacuum. Therefore, we continue with a more detailed study of the light stau parameter space.

#### 4.2 Constraining the light stau parameter space

Light staus in the MSSM are particularly interesting because if their mass is sufficiently close to the mass of a neutralino LSP then co-annihilation between the staus and the neutralinos can explain the observed dark matter relic density [79–81]. The measured dark matter relic density in the  $3\sigma$  range of Planck [82] is  $\Omega h^2 = 0.1199 \pm 0.081$ . This demands a mass splitting of at most a few GeV between the stau and neutralino. To obtain this, usually large values of  $|A_0|$  and/or  $\tan\beta$  are needed. However, as we have seen, this is exactly the parameter range which is in particular danger of CCB minima due to stau VEVs. As a starting point we can use the results of figure 4 for the minimal value of  $A_0$  and



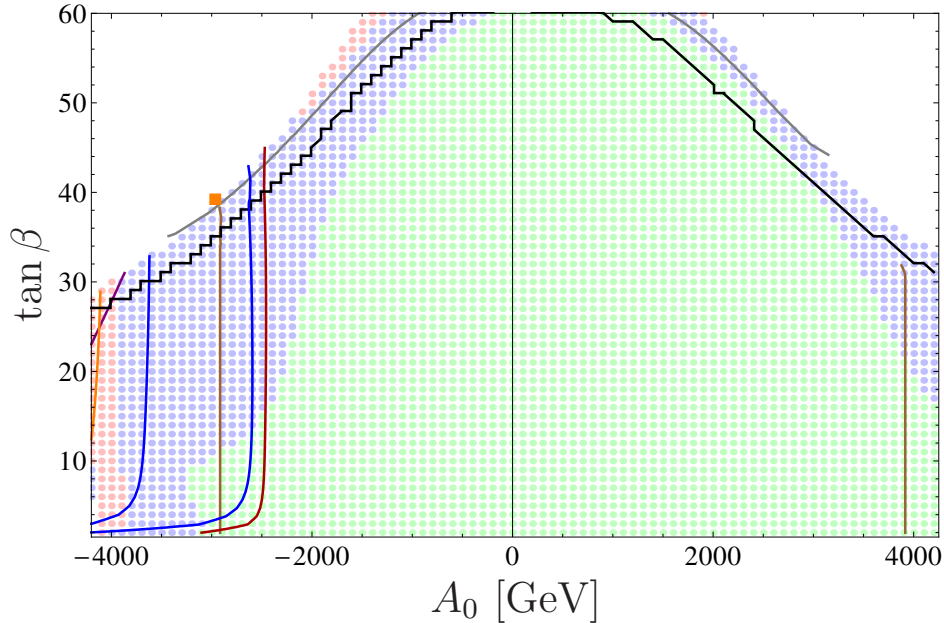


**Figure 5.** Vacuum stability in the  $(A_0, \tan \beta)$ -plane for fixed values of  $M_0 = M_{1/2} = 1$  TeV and  $\mu > 0$ . The color coding is as in figure 1 and in section 2: points on the other side of the solid lines from the  $A_0 = 0$  axis fail the corresponding conditions and so would be identified as having CCB minima deeper than the DSB minima. The left-most of the blue lines corresponds to taking  $0.85^2$  in condition (2.13), and the other to  $0.65^2$ . The single orange square corresponds to a projection of the best-fit point of Ref. [18] for reference. Points below the dotted line have the lightest neutralino as the LSP.

translate this into a lower limit on the light stau mass for given parameters, which we show in figure 6. This shows that for  $M_{1/2} > 500$  GeV and stau masses below 500 GeV, deeper vacua are possible, and therefore a careful test of the vacuum stability is required.

However, parameter points with CCB minima deeper than the DSB minimum may still be viable if the tunneling time is sufficiently long. We exemplify this in figure 7, where we plot the stable and metastable areas in the  $(M_{1/2}, M_0)$  plane for  $\tan \beta = 40$  and  $A_0 = 3000$  GeV. Note that this is the same area which has been studied in Ref. [81]. It is also depicted that only a very tiny region of the entire plane would be forbidden by the rules presented in section 2 (including some stable points that would be mistakenly excluded), while our full numerical checks show that the excluded parameter region is much larger if one demands conservatively that the DSB minimum is the global minimum. On the right-hand side of figure 7, we zoom into the area with sufficiently large stau co-annihilation to explain the dark matter abundance. Here, we used *MicrOmegas* 2.4.5 [83, 84] together with the *SUSY Toolbox* [85] to calculate the relic density. Fortunately for advocates of the stau co-annihilation region, the tunneling time out of the DSB false vacuum is phenomenologically acceptably long over the entire region shown in figure 7.

In figure 8, we provide another example to point out that vacuum stability in the context of stau co-annihilation is a severe issue which has not been taken into account to the demanded level. Here we show the  $(M_0, A_0)$ -plane around the best-fit point found in Ref. [18]. In this plane, the main part of the co-annihilation strip, including the best-fit point itself, would be ruled out by demanding that the DSB vacuum is absolutely stable, though it is allowed if one only demands that it has a lifetime

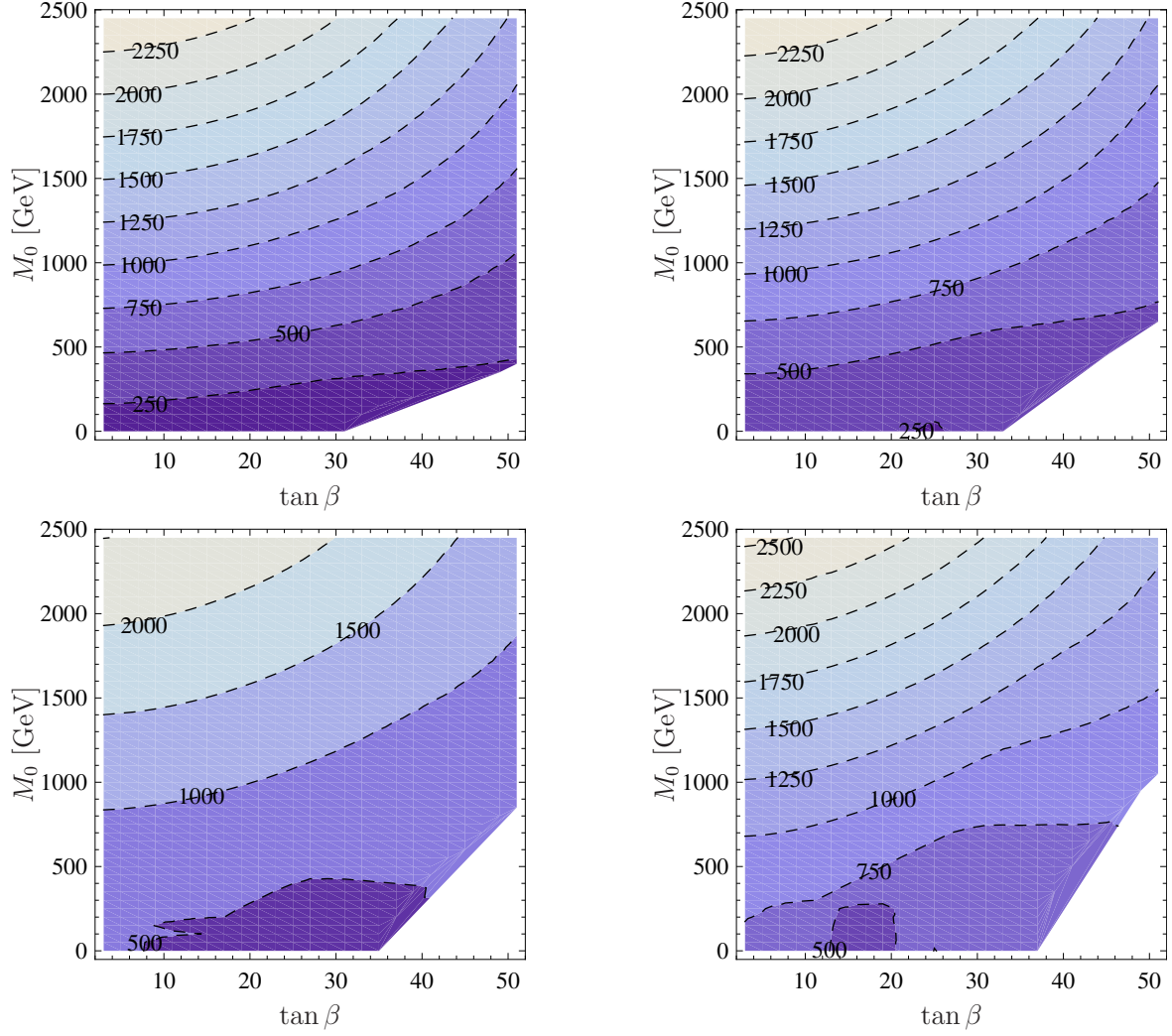


**Figure 6.** Minimal stau mass in the  $(\tan\beta, M_0)$  plane to have a stable DSB vacuum for  $A_0 < 0$ . We used  $\mu > 0$  and  $M_{1/2} = 500$  GeV (upper left),  $M_{1/2} = 1000$  GeV (upper right),  $M_{1/2} = 1500$  GeV (lower left) and  $M_{1/2} = 2000$  GeV (lower right).

of at least three gigayears. Again, the rules from section 2 do not constrain the interesting region at all, except for condition (2.11), which also excludes stable regions. It is interesting to note that the only condition which happens to constrain even partially any interesting region in our scans is one that is being used inappropriately, as it is being applied to parameters where the assumptions for its derivation are invalid, and it is no surprise that it also excludes stable points.

Lastly, we would like to discuss another comparison between the results of the full-fledged analysis and the analytical approximations of section 2. In figure 9, we show the light stau masses as well as the vacuum stability in the  $(M_0, A_0)$  plane for  $\tan\beta = 40$  and 50.  $M_{1/2}$  was fixed to 1 TeV. For  $\tan\beta = 40$ , the approximations totally fail, with the exception of (2.11), which is at least not totally useless even though it really should only apply for  $Y_t \ll 1$ . All of the other conditions would lie in the

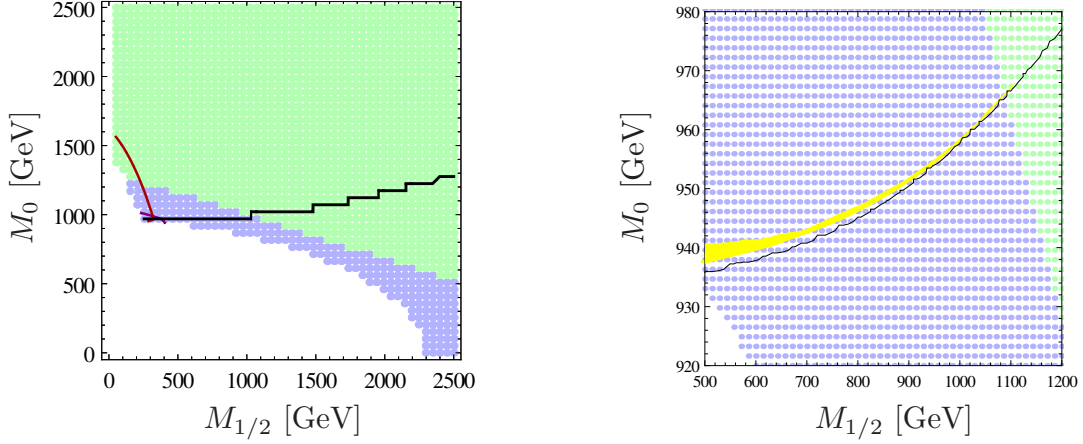


**Figure 7.** Dark matter and vacuum stability in the  $(M_{1/2}, M_0)$  plane with  $A_0 = 3$  TeV,  $\mu > 0$  and  $\tan \beta = 40$ . On the left, the dashed black line shows the transition between a neutralino and stau LSP (stau LSP beneath the line); on the right we zoom in on the interesting range for dark matter: the yellow bands show the region where  $\Omega h^2 = 0.1199 \pm 0.081$ . The constraints from vacuum stability allowing for stop and stau VEVs are indicated. The color coding is as in figure 1 and in section 2: points to the left of the solid lines fail the corresponding conditions. Here and in subsequent figures, physical quantities such as the dark matter relic density and particles masses are taken to be evaluated at the DSB vacuum regardless of its stability.

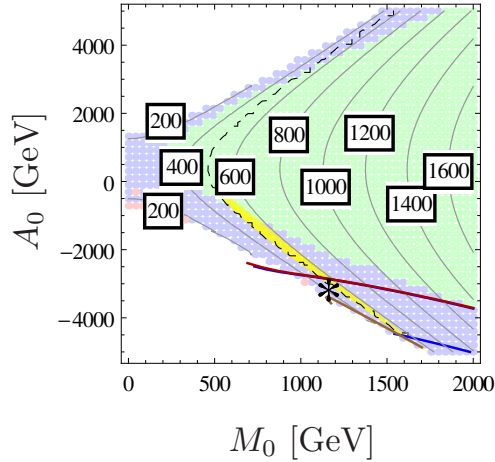


**Figure 8.** Mass of the light stau and vacuum stability in the  $(M_0, A_0)$  plane with  $M_{1/2} = 1167.4$  GeV,  $\mu > 0$  and  $\tan \beta = 39.3$ . In the yellow region, the abundance of the LSP is in agreement with dark matter constraints, and the dashed line shows the transition to a charged LSP. The color coding is as in figure 1 and in section 2: points below the solid lines fail the corresponding conditions. The lower blue line corresponds to condition (2.13) taking  $0.85^2$ , the upper, which is almost exactly degenerate with the dark red line of condition (2.11), corresponds to taking  $0.65^2$ . The star indicates the best-fit point according to Ref. [18].

white region, which is already excluded by tachyonic states at the DSB vacuum. For  $\tan \beta = 50$  the

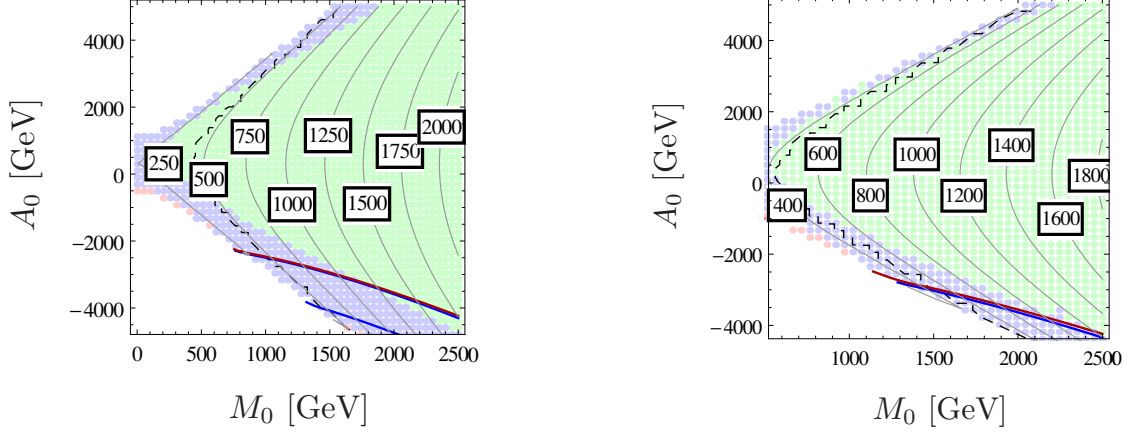


**Figure 9.** Vacuum stability and stau masses in the  $(M_0, A_0)$  plane for fixed  $M_{1/2} = 1$  TeV,  $\mu > 0$  and  $\tan \beta = 40$  (left) or  $\tan \beta = 50$  (right). The dashed black line shows the transition to a charged LSP (neutralino LSP to the right of the line). The color coding is as in figure 1 and in section 2: points to the left of the solid lines fail the corresponding conditions. As in figure 8, the blue line for condition (2.13) with  $0.65^2$  is almost degenerate with the dark red line of condition (2.11) and the line for  $0.85^2$  only excludes points with even more negative  $A_0$  (and is not visible on the right).

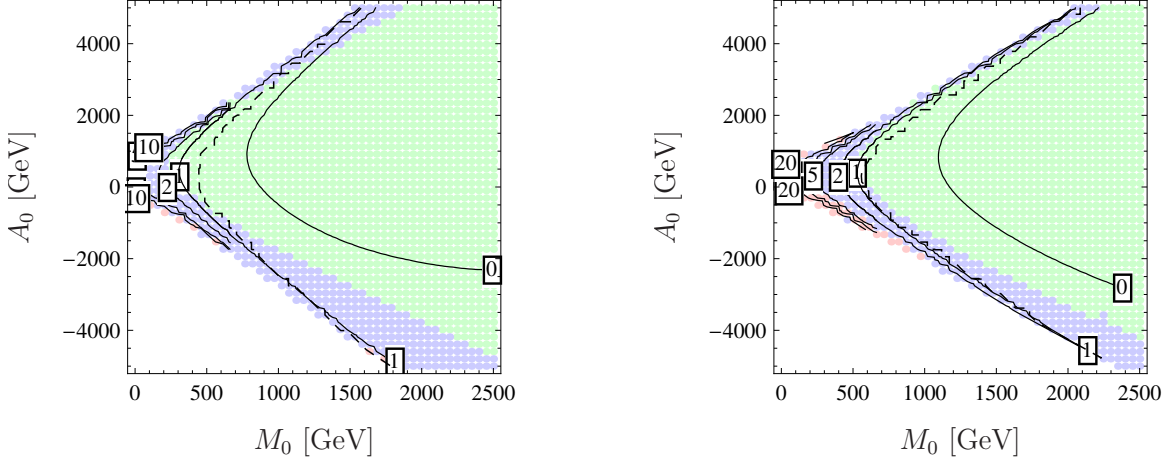


**Figure 10.** The enhancement of the branching ratio of the lighter Higgs boson relative to the SM prediction, given in per-cent, in the  $(M_0, A_0)$  plane for fixed  $M_{1/2} = 1$  TeV,  $\mu > 0$  and  $\tan \beta = 40$  (left) or  $\tan \beta = 50$  (right). The contour labeled 0 shows where the branching ratio is equal to that of the SM, the one labeled 1 shows where it is 1% greater than in the SM, and so on. The dashed black line shows the transition to a charged LSP (neutralino LSP to the right of the line). The color coding is as in figure 1.

situation is only slightly better: tiny parts of the small  $M_0$  areas are in conflict with conditions (2.14). However, the main part of the metastable vacua would also survive all cuts applying those rules (with (2.11) performing less well). Hence, for large  $\tan \beta$  and reasonable SUSY spectra above the LHC exclusion limits, one can not rely at all on conditions (2.9), (2.10), (2.12), (2.14) or (2.15).

One might wonder whether the lower bounds on the mass of the lightest stau by demanding stability of the DSB vacuum could restrict parameter regions of the CMSSM where the branching ratio of the lighter neutral Higgs boson to a pair of photons is enhanced relative to the SM prediction, as is currently weakly favored by Atlas [86]. Certainly light stau masses are required, close to the LEP limit of  $\mathcal{O}(100 \text{ GeV})$  [50, 87], and restrictions of the pMSSM parameter space has been discussed to some extent in the literature [51]. We show in figure 10 the contours of enhancement of the ratio for two particular slices of the parameter space. As can be seen, enhancements of up to 20% can be achieved, and that the tunneling time to CCB vacua is a very relevant constraint for the parameter region, but the regions plotted at least are not phenomenologically interesting anyway as the stau is much lighter than the lightest neutralino there, and the regions where the neutralino is a valid dark matter candidate also have very little enhancement of the diphoton branching ratio. This might favor additional light charged fermions in extended SUSY models to explain the possible enhancement [88–90], or very light charginos in the MSSM below 100 GeV which could escape all present collider limits [91].

### 4.3 Constraining the light stop parameter space

The stops play an important role in the MSSM as they are needed to push the mass of the light Higgs to about 125 GeV via radiative corrections [11–15]. For this one needs either rather heavy stops, as for example in gauge-mediated SUSY-breaking [13, 92] or large  $|A_t|$  to obtain the maximal mixing scenario [11, 93, 94]. A rough estimate is given by  $A_t \simeq 0.2A_0 - 2M_{1/2}$  [95] causing the observed preference for negative  $A_0$ . Moreover,  $|A_0| \simeq 2M_0$  [94] is required implying the peril of developing CCB minima.

The information of figure 4 can be translated into a lower limit on the stop mass by demanding a stable DSB vacuum which is given in figure 11. We see that for small  $M_{1/2}$ , this condition excludes light stop masses of the order of current lower limit from direct searches of about 600 GeV [96]. However, for larger values of  $M_{1/2}$ , the lower mass limit is much stronger: in the TeV range. Furthermore, our limits are independent of the mass splitting between the stop and the lightest neutralino or chargino.

In addition to offering a new particle accessible to the LHC possibly motivated by naturalness arguments [97, 98], a stop NLSP could also give the correct neutralino abundance to explain the dark matter relic density. Even though stop co-annihilation usually works very efficiently for a larger mass splitting between the NSLP and LSP compared to the case for staus, the stops still have to be sufficiently light [99]. Recent benchmark points for this scenario have been proposed in Ref. [100]. A scan around their benchmark point 5.1 ( $M_0 = 2667 \text{ GeV}$ ,  $M_{1/2} = 933 \text{ GeV}$ ,  $\tan\beta = 8.52$ ,  $\mu < 0$ ,  $A_0 = -6444 \text{ GeV}$ ) in the  $(M_{1/2}, M_0)$  plane is shown in figure 12, where we give the contour lines of the stop mass as well as the vacuum stability. The entire region which contains the stop coannihilation region has deeper CCB vacua and at least half of the points would tunnel from the DSB vacuum to CCB minima with an unacceptably short tunneling time. Note this can be a severe problem not only for stop coannihilation in the CMSSM, but also for pMSSM benchmark scenarios such as those discussed in Ref. [101]. One solution to resurrect stop co-annihilation would be to go to much larger mass spectra; e.g. the BP 5.2 of Ref. [100] with  $m_{\tilde{\chi}_1^0} = 1 \text{ TeV}$  seems to be stable against tunneling to CCB minima.

We conclude this section with a comparison between our numerical results and the thumb rules given in the literature. We show in figure 13 the mass of the light stop and the vacuum stability in the  $(M_0, A_0)$  plane for  $M_{1/2} = 1 \text{ TeV}$  and  $\tan\beta = 2$  or 10. As can be easily seen, the conditions are rather irrelevant except for misusing conditions (2.11) and (2.12).

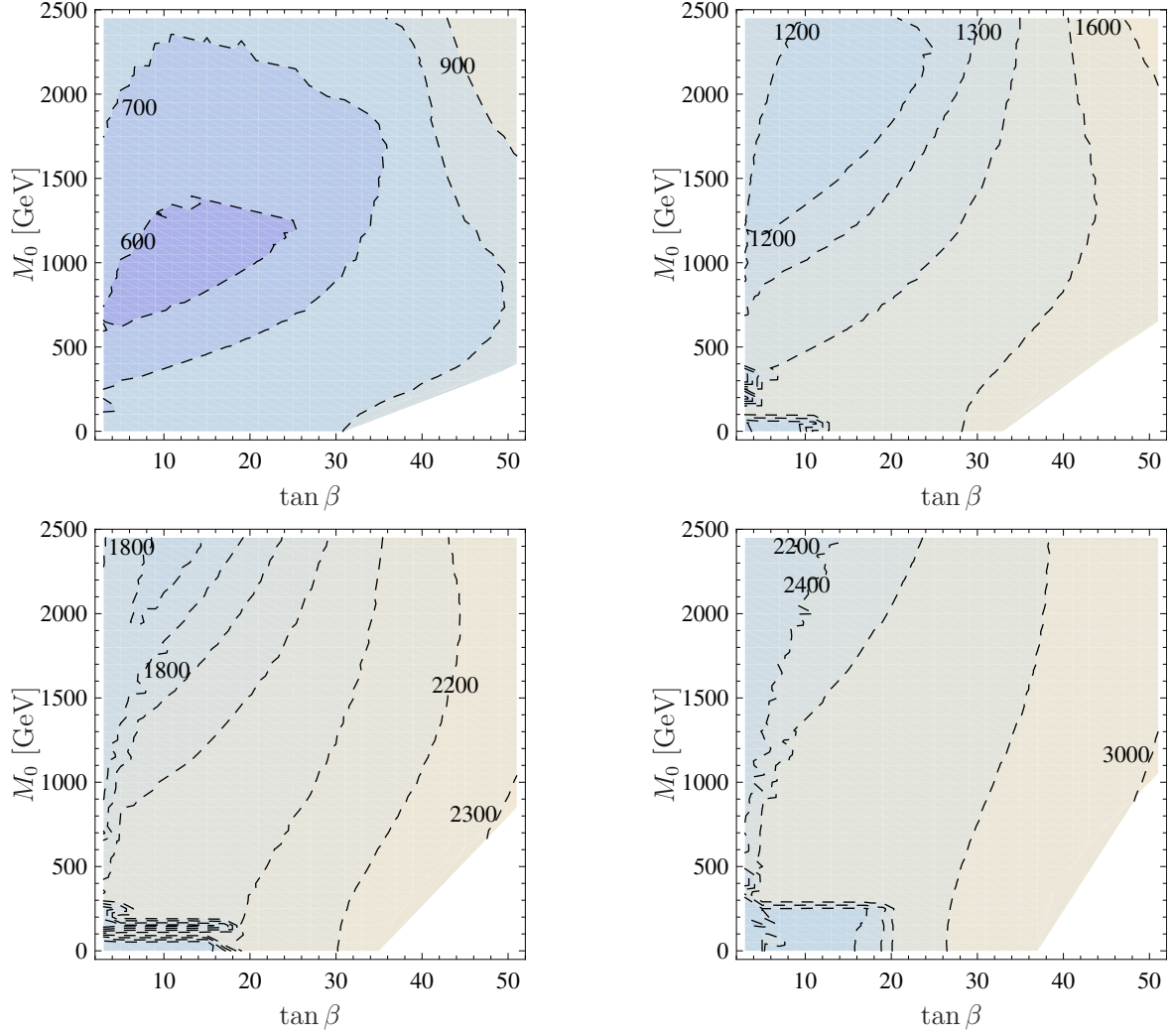


**Figure 11.** Minimal stop mass in the  $(\tan\beta, M_0)$  plane to have a stable DSB vacuum for  $A_0 < 0$ . We used  $\mu > 0$  and  $M_{1/2} = 500$  GeV (upper left),  $M_{1/2} = 1000$  GeV (upper right),  $M_{1/2} = 1500$  GeV (lower left) and  $M_{1/2} = 2000$  GeV (lower right).

In general, the condition of stable or at least long-lived vacua in the case of small  $\tan\beta$  and for negative  $A_0$  puts severe limits on the mass of the light stop, and rapid tunneling times can rule out light stops in the CMSSM depending on the value of  $M_{1/2}$ .

#### 4.4 Constraining the parameter space of $m_h \simeq 125$ GeV

The measurement of  $m_h \simeq 125.5$  GeV [4, 5] implies a powerful constraint on the parameter space of supersymmetric models due to the need for large radiative corrections. To get loop contributions which are large enough to increase the tree-level Higgs mass of  $m_h^{(TL)} \leq m_Z$  by more than 30 GeV, one needs a large mass splitting in the stop sector, i.e.  $|A_0|$  must usually be large in comparison to  $M_0$ , see Refs. [93, 102–105] and references therein. At the one-loop level, the corrections are maximized



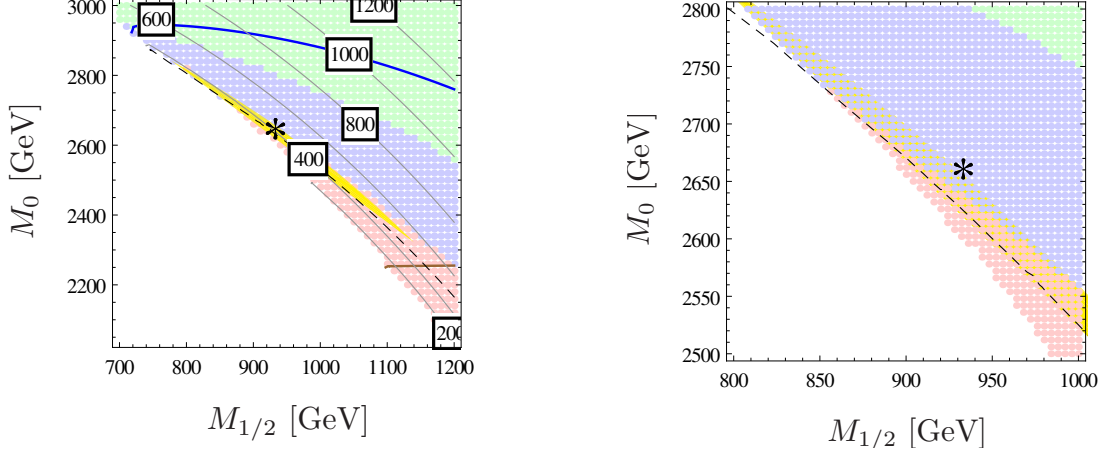


**Figure 12.** Mass of the light stop and vacuum stability in the  $(M_{1/2}, M_0)$  plane with  $A_0 = -6444$  GeV,  $\mu < 0$  and  $\tan \beta = 8.52$ . The dashed line shows the transition to a charged LSP (neutralino LSP to the right of the line). The color coding is as in figure 1 and in section 2: points below the solid lines fail the corresponding conditions. In the yellow region,  $\Omega h^2$  is in agreement with dark matter constraints (as in figure 8). The star indicates the benchmark point 5.1 of Ref. [100]. The reason that this point is not in the strip with the correct dark matter abundance is that different SM input parameters were used in Ref. [100] in comparison to eq. (3.1):  $m_t = 174.3$  GeV,  $\alpha_S = 0.1172$  and  $m_b(m_b) = 4.25$  GeV. The line showing the division between passing and failing condition 2.13 using  $0.65^2$  does not appear on this plot, but over-zealously would exclude the entire region shown, while taking  $0.65^2$  would only exclude every point with  $M_0 \lesssim 2900$  GeV.

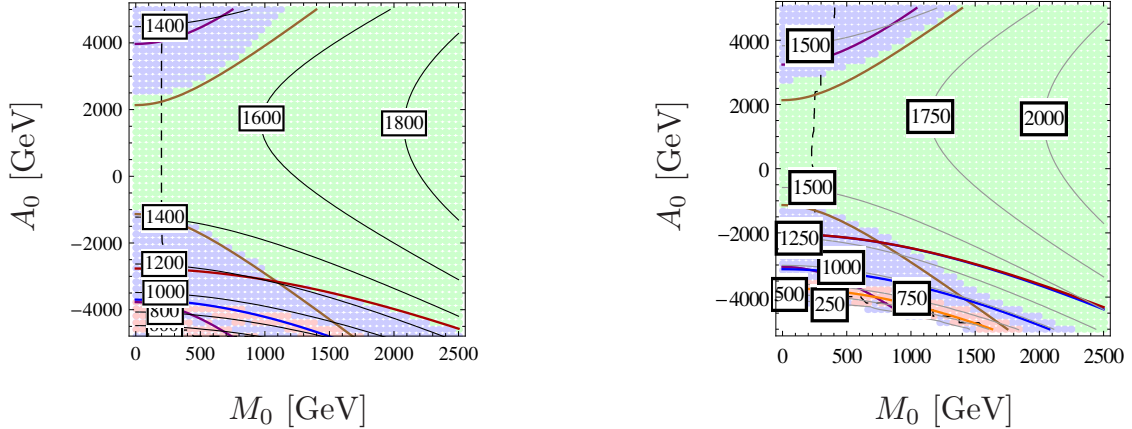


**Figure 13.** Stop mass and vacuum stability in the  $(M_0, A_0)$  plane. We used  $M_{1/2} = 1$  TeV,  $\mu > 0$  and  $\tan \beta = 2$  (left) or  $\tan \beta = 10$  (right). The color coding is as in figure 1 and in section 2: points to the left of the solid lines fail the corresponding conditions. Again, there is a degeneracy between the more exclusive blue line of condition (2.13) with the dark red line of condition (2.11). Points to the left of the dashed line also have charged LSPs.

for  $X_t = A_t - \mu / \tan \beta \simeq \sqrt{6} M_S$  where  $M_S$  is the average stop mass. Taking two-loop corrections into account, this gets shifted to  $X_t \simeq 2 M_S$  [94].



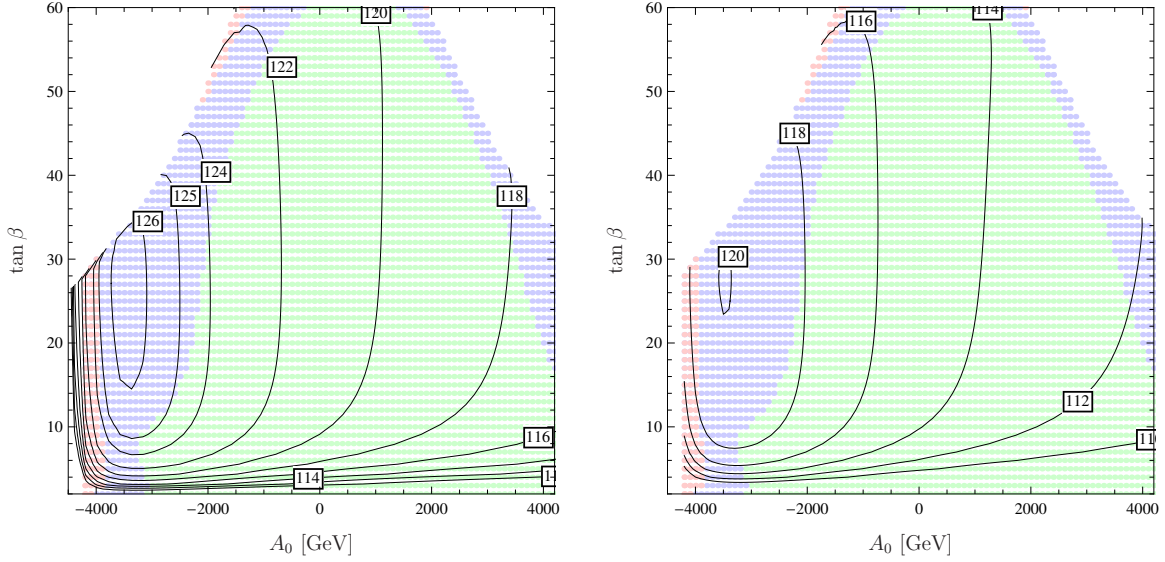


**Figure 14.** Vacuum stability and the Higgs mass in the  $(A_0, \tan \beta)$  plane for fixed  $M_0 = M_{1/2} = 1$  TeV and  $\mu > 0$ . On the left, the leading two-loop corrections at the DSB minimum have been taken into account, while on the right, the mass of the lighter Higgs boson is shown only at one-loop order. The color code is the same as in figure 1.

However, as we have seen in the last sections, these are exactly the regions in the CMSSM parameter space which often suffer from a CCB minimum deeper than the DSB minimum. To demonstrate this, we take parameter planes discussed previously and show the calculated mass of the lightest Higgs boson. While the vacuum stability was calculated using the one-loop effective potential, these Higgs masses are based on a full diagrammatic one-loop calculation including the effects of the external momenta [106] and, in addition, the known two-loop corrections are included [65–68]. For completeness, we also show the mass of the lighter Higgs boson evaluated at one-loop order beside each plot.

One might wonder about whether two-loop effects are important for the evaluation of the stability of the DSB vacuum, given that they are critical for obtaining the experimental value of the mass of the Higgs boson in the CMSSM. Unfortunately **Vevacious** is currently restricted to one-loop order, and only the leading two-loop corrections at the DSB vacuum in the special case of the MSSM are known, let alone the full two-loop expression for arbitrary field configurations. However, given that the two-loop corrections to the Higgs mass-squared are of the order of 10% compared to the one-loop corrections being of order 100%, along with the indications from figure 3 that loop corrections play a subdominant role if the scale is chosen judiciously, as expected, as the usual SUSY scale, it would seem that the loop expansion converges well and the higher orders should not affect the results substantially.

To show how serious the Higgs mass constraint in combination with vacuum stability is, we start with moderate SUSY masses and put  $M_0 = M_{1/2} = 1$  TeV. The Higgs mass and the vacuum stability in the  $(A_0, \tan \beta)$  plane is shown in figure 14. We see that nearly the entire line where  $m_h = 125$  GeV is located in a range with charge- or color-breaking minima deeper than the DSB minima.

To test if the tension between the vacuum stability and the Higgs mass relaxes in the case of heavier SUSY spectra, we consider in figure 15 the  $(M_0, A_0)$  plane and allow  $M_0$  up to 2.5 TeV. In addition, we used  $M_{1/2} = 1$  TeV,  $\mu > 0$  and  $\tan \beta = 10, 40$ . For both values of  $\tan \beta$ , the correct Higgs

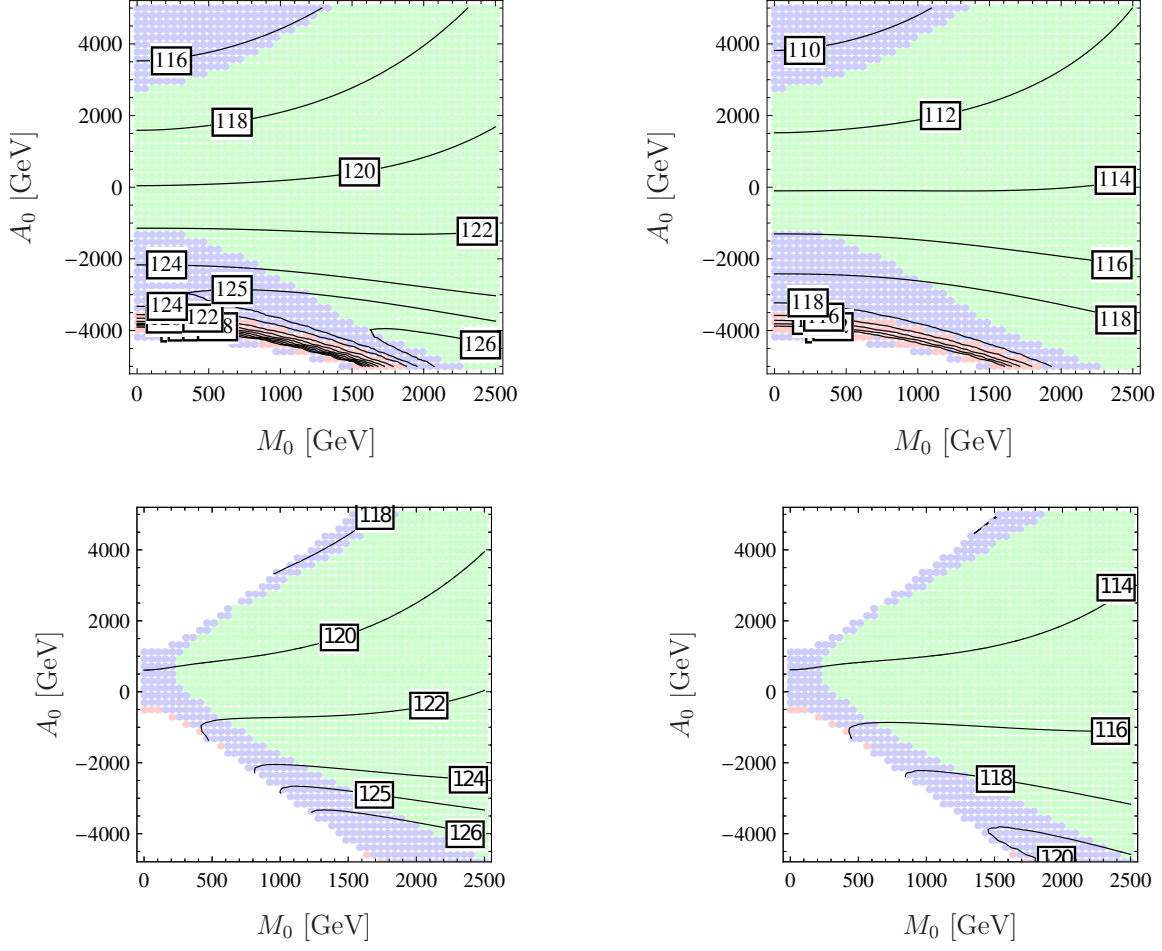


**Figure 15.** Vacuum stability and the Higgs mass in the  $(M_0, A_0)$  plane for fixed  $M_{1/2} = 1$  TeV,  $\mu > 0$  and  $\tan \beta = 10$  (upper) or  $\tan \beta = 40$  (lower). On the left, the leading two-loop corrections to the mass of the lighter Higgs boson have been taken into account, on the right, only the mass at one-loop order is shown. The color code is the same as in figure 1.

mass can only be reached for large negative values of  $A_0$ , as expected. Especially for small  $M_0$ , the ratio  $|A_0/M_0|$  must be huge to push the Higgs mass to the desired value. As a consequence, all points with  $m_h > 124$  GeV are in an area with CCB minima deeper than the DSB minima for  $M_0 < 900$  GeV ( $\tan \beta = 10$ ) respectively  $M_0 < 1200$  GeV ( $\tan \beta = 40$ ). The lower bound on  $M_0$  increases by about 300 GeV if one demands  $m_h \geq 125$  GeV. Only for larger  $M_0$  it is possible to find points with the Higgs mass in the correct range and a DSB vacuum stable against tunneling to CCB vacua.

## 5 Discussion and conclusion

As we have shown, the calculation of tunneling times from a phenomenological minimum to charge- and/or color-breaking minima can be taken as a new constraint for excluding unphysical parameter points.

A lot of effort has been spent in the literature to find best-fit points that consider a vast amount of phenomenology data. However, vacuum stability is either not considered or introduced by the use of one or more of the conditions which we have shown to be obsolete. This is not limited to the CMSSM: for instance, the general MSSM points given by the ‘natural SUSY’ benchmark of [107] and benchmark ‘I’ of [101] suffer from unacceptably short tunneling times to CCB minima with stop VEVs.

We have discussed the impact of the vacuum stability on the parameter space of the CMSSM. The difference to previous studies is that we have used a fully numerical approach ensuring that all deeper charge- and color-breaking minima at tree level are found. In addition, the inclusion of the one-loop corrections to the effective potential reduced the uncertainty from the scale at which the potential is evaluated. It turned out that approximate thumb rules which have been analytically derived in the literature do not exclude much of the relevant parameter space where the DSB vacuum suffers from a rapid decay into a deeper minimum with broken  $U(1)_{EM}$  and maybe even  $SU(3)_c$ . This happens especially in areas of the parameter space with a large stau and/or stop mass splitting. However, these are the regions which have been considered as phenomenologically preferred since they could explain the abundance of dark matter due to a co-annihilation mechanism. It has been shown that many regions discussed in this context are already ruled out if one includes the constraint that the DSB vacuum must be stable or at least long-lived metastable.

In addition, the large stop mass splitting is also needed to explain the measurement of the Higgs mass within the CMSSM. We found that for SUSY masses in the lower TeV range hardly any region in the CMSSM can be found which leads to a Higgs mass of 125 GeV or above without suffering from CCB global minima.

## Acknowledgments

The authors would like to thank Sasha Belyaev for useful discussions on the limits of the stau co-annihilation strip. This work has been supported by the DFG, research training group GRK 1147 and project No. PO-1337/2-1. FS is supported by the BMBF PT DESY Verbundprojekt 05H2013-THEORIE “Vergleich von LHC-Daten mit supersymmetrischen Modellen”.

## References

- [1] S. Glashow, *Partial Symmetries of Weak Interactions*, Nucl.Phys. **22** (1961) 579–588.
- [2] S. Weinberg, *A Model of Leptons*, Phys.Rev.Lett. **19** (1967) 1264–1266.
- [3] A. Salam, *Weak and Electromagnetic Interactions*, in Elementary Particle Theory, ed. N. Svartholm (Almqvist and Wiksells, Stockholm, 1968) (1968) 367–377.
- [4] **ATLAS Collaboration**, G. Aad et al., *Observation of a new particle in the search for the Standard Model Higgs boson with the ATLAS detector at the LHC*, Phys.Lett. **B716** (2012) 1–29, [[arXiv:1207.7214](#)].
- [5] **CMS Collaboration**, S. Chatrchyan et al., *Observation of a new boson at a mass of 125 GeV with the CMS experiment at the LHC*, Phys.Lett. **B716** (2012) 30–61, [[arXiv:1207.7235](#)].
- [6] S. P. Martin, *A Supersymmetry primer*, [hep-ph/9709356](#).
- [7] G. R. Farrar and P. Fayet, *Phenomenology of the Production, Decay, and Detection of New Hadronic States Associated with Supersymmetry*, Phys.Lett. **B76** (1978) 575–579.

- [8] B. Allanach, D. P. George, and B. Gripaios, *The dark side of the  $\mu$ : on multiple solutions to renormalisation group equations, and why the CMSSM is not necessarily being ruled out*, JHEP **1307** (2013) 098, [[arXiv:1304.5462](#)].
- [9] K. A. Olive and M. Srednicki, *New Limits on Parameters of the Supersymmetric Standard Model from Cosmology*, Phys.Lett. **B230** (1989) 78.
- [10] J. R. Ellis, T. Falk, and K. A. Olive, *Neutralino - Stau coannihilation and the cosmological upper limit on the mass of the lightest supersymmetric particle*, Phys.Lett. **B444** (1998) 367–372, [[hep-ph/9810360](#)].
- [11] P. Draper, P. Meade, M. Reece, and D. Shih, *Implications of a 125 GeV Higgs for the MSSM and Low-Scale SUSY Breaking*, Phys.Rev. **D85** (2012) 095007, [[arXiv:1112.3068](#)].
- [12] S. Heinemeyer, O. Stal, and G. Weiglein, *Interpreting the LHC Higgs Search Results in the MSSM*, Phys.Lett. **B710** (2012) 201–206, [[arXiv:1112.3026](#)].
- [13] F. Brümmer, S. Kraml, and S. Kulkarni, *Anatomy of maximal stop mixing in the MSSM*, JHEP **1208** (2012) 089, [[arXiv:1204.5977](#)].
- [14] A. Djouadi and J. Quevillon, *The MSSM Higgs sector at a high  $M_{SUSY}$ : reopening the low  $\tan\beta$  regime and heavy Higgs searches*, [arXiv:1304.1787](#).
- [15] A. Arbey, M. Battaglia, A. Djouadi, and F. Mahmoudi, *An update on the constraints on the phenomenological MSSM from the new LHC Higgs results*, Phys.Lett. **B720** (2013) 153–160, [[arXiv:1211.4004](#)].
- [16] E. Arganda, J. L. Diaz-Cruz, and A. Szyrkman, *Decays of  $H^0/A^0$  in supersymmetric scenarios with heavy sfermions*, Eur.Phys.J. **C73** (2013) 2384, [[arXiv:1211.0163](#)].
- [17] M. Citron, J. Ellis, F. Luo, J. Marrouche, K. Olive, et al., *The End of the CMSSM Coannihilation Strip is Nigh*, Phys.Rev. **D87** (2013) 036012, [[arXiv:1212.2886](#)].
- [18] P. Bechtle, T. Bringmann, K. Desch, H. Dreiner, M. Hamer, et al., *Constrained Supersymmetry after two years of LHC data: a global view with Fittino*, JHEP **1206** (2012) 098, [[arXiv:1204.4199](#)].
- [19] H. P. Nilles, M. Srednicki, and D. Wyler, *Weak Interaction Breakdown Induced by Supergravity*, Phys.Lett. **B120** (1983) 346.
- [20] L. Alvarez-Gaume, J. Polchinski, and M. B. Wise, *Minimal Low-Energy Supergravity*, Nucl.Phys. **B221** (1983) 495.
- [21] J. Derendinger and C. A. Savoy, *Quantum Effects and  $SU(2) \times U(1)$  Breaking in Supergravity Gauge Theories*, Nucl.Phys. **B237** (1984) 307.
- [22] M. Claudson, L. J. Hall, and I. Hinchliffe, *Low-Energy Supergravity: False Vacua and Vacuum Predictions*, Nucl.Phys. **B228** (1983) 501.
- [23] C. Kounnas, A. Lahanas, D. V. Nanopoulos, and M. Quiros, *Low-Energy Behavior of Realistic Locally Supersymmetric Grand Unified Theories*, Nucl.Phys. **B236** (1984) 438.
- [24] M. Drees, M. Glück, and K. Grassie, *A NEW CLASS OF FALSE VACUA IN LOW-ENERGY  $N=1$  SUPERGRAVITY THEORIES*, Phys.Lett. **B157** (1985) 164.
- [25] J. Gunion, H. Haber, and M. Sher, *Charge / Color Breaking Minima and  $a$ -Parameter Bounds in Supersymmetric Models*, Nucl.Phys. **B306** (1988) 1.
- [26] H. Komatsu, *NEW CONSTRAINTS ON PARAMETERS IN THE MINIMAL SUPERSYMMETRIC MODEL*, Phys.Lett. **B215** (1988) 323.

- [27] P. Langacker and N. Polonsky, *Implications of Yukawa unification for the Higgs sector in supersymmetric grand unified models*, Phys.Rev. **D50** (1994) 2199–2217, [[hep-ph/9403306](#)].
- [28] J. Casas, A. Lleyda, and C. Muñoz, *Strong constraints on the parameter space of the MSSM from charge and color breaking minima*, Nucl.Phys. **B471** (1996) 3–58, [[hep-ph/9507294](#)].
- [29] J. Casas and S. Dimopoulos, *Stability bounds on flavor violating trilinear soft terms in the MSSM*, Phys.Lett. **B387** (1996) 107–112, [[hep-ph/9606237](#)].
- [30] A. Kusenko, P. Langacker, and G. Segre, *Phase transitions and vacuum tunneling into charge and color breaking minima in the MSSM*, Phys.Rev. **D54** (1996) 5824–5834, [[hep-ph/9602414](#)].
- [31] S. Abel and C. A. Savoy, *On metastability in supersymmetric models*, Nucl.Phys. **B532** (1998) 3–27, [[hep-ph/9803218](#)].
- [32] R. Kuchimanchi and R. N. Mohapatra, *No parity violation without  $r$ -parity violation*, Phys. Rev. D **48** (Nov, 1993) 4352–4360.
- [33] A. J. Bordner, *Parameter bounds in the supersymmetric standard model from charge / color breaking vacua*, [[hep-ph/9506409](#)].
- [34] P. Ferreira, *A Full one loop charge and color breaking effective potential*, Phys.Lett. **B509** (2001) 120–130, [[hep-ph/0008115](#)].
- [35] A. Riotto and E. Roulet, *Vacuum decay along supersymmetric flat directions*, Phys.Lett. **B377** (1996) 60–66, [[hep-ph/9512401](#)].
- [36] A. Kusenko and P. Langacker, *Is the vacuum stable?*, Phys.Lett. **B391** (1997) 29–33, [[hep-ph/9608340](#)].
- [37] T. Falk, K. A. Olive, L. Roszkowski, A. Singh, and M. Srednicki, *Constraints from inflation and reheating on superpartner masses*, Phys.Lett. **B396** (1997) 50–57, [[hep-ph/9611325](#)].
- [38] J. R. Ellis, J. Giedt, O. Lebedev, K. Olive, and M. Srednicki, *Against Tachyophobia*, Phys.Rev. **D78** (2008) 075006, [[arXiv:0806.3648](#)].
- [39] M. Maniatis, A. von Manteuffel, and O. Nachtmann, *Determining the global minimum of Higgs potentials via Groebner bases: Applied to the NMSSM*, Eur.Phys.J. **C49** (2007) 1067–1076, [[hep-ph/0608314](#)].
- [40] J. Gray, Y.-H. He, A. Ilderton, and A. Lukas, *STRINGVACUA: A Mathematica Package for Studying Vacuum Configurations in String Phenomenology*, Comput.Phys.Commun. **180** (2009) 107–119, [[arXiv:0801.1508](#)].
- [41] L. J. Huang and T.-Y. Li, *Parallel homotopy algorithm for symmetric large sparse eigenproblems*, Journal of Computational and Applied Mathematics **60** (1995), no. 1–2 77 – 100. Proceedings of the International Meeting on Linear/Nonlinear Iterative Methods and Verification of Solution.
- [42] A. Sommese and C. Wampler, “The numerical solution of systems of polynomials arising in engineering and science. 2005.”
- [43] T. Li, *Numerical solution of polynomial systems by homotopy continuation methods*, Handbook of numerical analysis **11** (2003) 209–304.
- [44] J. Camargo-Molina, B. O’Leary, W. Porod, and F. Staub, *Vevacious: A Tool For Finding The Global Minima Of One-Loop Effective Potentials With Many Scalars*, [[arXiv:1307.1477](#)].
- [45] H. Baer, M. Brhlik, and D. Castaño, *Constraints on the minimal supergravity model from nonstandard vacua*, Phys.Rev. **D54** (1996) 6944–6956, [[hep-ph/9607465](#)].

- [46] A. Strumia, *Charge and color breaking minima and constraints on the MSSM parameters*, Nucl.Phys. **B482** (1996) 24–38, [[hep-ph/9604417](#)].
- [47] D. Cerdeno, E. Gabrielli, M. Gomez, and C. Muñoz, *Neutralino nucleon cross-section and charge and color breaking constraints*, JHEP **0306** (2003) 030, [[hep-ph/0304115](#)].
- [48] U. Ellwanger and C. Hugonie, *Constraints from charge and color breaking minima in the  $(M+1)$ SSM*, Phys.Lett. **B457** (1999) 299–306, [[hep-ph/9902401](#)].
- [49] C. Le Mouél, *Charge and color breaking conditions associated to the top quark Yukawa coupling*, Phys.Rev. **D64** (2001) 075009, [[hep-ph/0103341](#)].
- [50] M. Carena, S. Gori, N. R. Shah, C. E. Wagner, and L.-T. Wang, *Light Stau Phenomenology and the Higgs  $\gamma\gamma$  Rate*, JHEP **1207** (2012) 175, [[arXiv:1205.5842](#)].
- [51] M. Carena, S. Gori, I. Low, N. R. Shah, and C. E. Wagner, *Vacuum Stability and Higgs Diphoton Decays in the MSSM*, [arXiv:1211.6136](#).
- [52] J. Hisano and S. Sugiyama, *Charge-breaking constraints on left-right mixing of stau's*, Phys.Lett. **B696** (2011) 92–96, [[arXiv:1011.0260](#)].
- [53] T. Kitahara and T. Yoshinaga, *Stau with Large Mass Difference and Enhancement of the Higgs to Diphoton Decay Rate in the MSSM*, JHEP **1305** (2013) 035, [[arXiv:1303.0461](#)].
- [54] H. Baer, F. E. Paige, S. D. Protopopescu, and X. Tata, *Simulating Supersymmetry with ISAJET 7.0 / ISASUSY 1.0*, [hep-ph/9305342](#).
- [55] F. E. Paige, S. D. Protopopescu, H. Baer, and X. Tata, *ISAJET 7.69: A Monte Carlo event generator for pp, anti-p p, and e+e- reactions*, [hep-ph/0312045](#).
- [56] B. Allanach, *SOFTSUSY: a program for calculating supersymmetric spectra*, Comput.Phys.Commun. **143** (2002) 305–331, [[hep-ph/0104145](#)].
- [57] W. Porod, *SPheno, a program for calculating supersymmetric spectra, SUSY particle decays and SUSY particle production at e+ e- colliders*, Comput. Phys. Commun. **153** (2003) 275–315, [[hep-ph/0301101](#)].
- [58] W. Porod and F. Staub, *SPheno 3.1: Extensions including flavour, CP-phases and models beyond the MSSM*, Comput.Phys.Commun. **183** (2012) 2458–2469, [[arXiv:1104.1573](#)].
- [59] A. Djouadi, J.-L. Kneur, and G. Moultaka, *SuSpect: A Fortran code for the supersymmetric and Higgs particle spectrum in the MSSM*, Comput.Phys.Commun. **176** (2007) 426–455, [[hep-ph/0211331](#)].
- [60] B. Allanach, S. Kraml, and W. Porod, *Theoretical uncertainties in sparticle mass predictions from computational tools*, JHEP **0303** (2003) 016, [[hep-ph/0302102](#)].
- [61] F. Staub, *SARAH*, [arXiv:0806.0538](#).
- [62] F. Staub, *From Superpotential to Model Files for FeynArts and CalcHep/CompHep*, Comput. Phys. Commun. **181** (2010) 1077–1086, [[arXiv:0909.2863](#)].
- [63] F. Staub, *Automatic Calculation of supersymmetric Renormalization Group Equations and Self Energies*, Comput. Phys. Commun. **182** (2011) 808–833, [[arXiv:1002.0840](#)].
- [64] F. Staub, *Linking SARAH and MadGraph using the UFO format*, [arXiv:1207.0906](#).
- [65] G. Degrandi, P. Slavich, and F. Zwirner, *On the neutral Higgs boson masses in the MSSM for arbitrary stop mixing*, Nucl.Phys. **B611** (2001) 403–422, [[hep-ph/0105096](#)].
- [66] A. Dedes and P. Slavich, *Two loop corrections to radiative electroweak symmetry breaking in the MSSM*, Nucl.Phys. **B657** (2003) 333–354, [[hep-ph/0212132](#)].



- [67] A. Brignole, G. Degrandi, P. Slavich, and F. Zwirner, *On the  $O(\alpha(t)^{**2})$  two loop corrections to the neutral Higgs boson masses in the MSSM*, Nucl.Phys. **B631** (2002) 195–218, [[hep-ph/0112177](#)].
- [68] A. Brignole, G. Degrandi, P. Slavich, and F. Zwirner, *On the two loop sbottom corrections to the neutral Higgs boson masses in the MSSM*, Nucl.Phys. **B643** (2002) 79–92, [[hep-ph/0206101](#)].
- [69] G. Degrandi and P. Slavich, *QCD Corrections in two-Higgs-doublet extensions of the Standard Model with Minimal Flavor Violation*, Phys.Rev. **D81** (2010) 075001, [[arXiv:1002.1071](#)].
- [70] F. Staub, *SARAH 4: A tool for (not only SUSY) model builders*, [arXiv:1309.7223](#).
- [71] S. P. Martin, *Two-loop effective potential for a general renormalizable theory and softly broken supersymmetry*, Phys. Rev. D **65** (May, 2002) 116003.
- [72] M. Hirsch, W. Porod, L. Reichert, and F. Staub, *Phenomenology of the minimal supersymmetric  $U(1)_{B-L} \times U(1)_R$  extension of the standard model*, Phys.Rev. **D86** (2012) 093018, [[arXiv:1206.3516](#)].
- [73] B. Allanach, M. Battaglia, G. Blair, M. S. Carena, A. De Roeck, et al., *The Snowmass points and slopes: Benchmarks for SUSY searches*, Eur.Phys.J. **C25** (2002) 113–123, [[hep-ph/0202233](#)].
- [74] L. Pearce, A. Kusenko, and R. Peccei, *Phenomenology of Supersymmetric Models with a Symmetry-Breaking Seesaw Mechanism*, Phys. Rev. D **88**, **075011** (2013) [[arXiv:1307.6157](#)].
- [75] A. Brignole, J. Espinosa, M. Quiros, and F. Zwirner, *Aspects of the electroweak phase transition in the minimal supersymmetric standard model*, Phys.Lett. **B324** (1994) 181–191, [[hep-ph/9312296](#)].
- [76] C. L. Wainwright, *CosmoTransitions: Computing Cosmological Phase Transition Temperatures and Bubble Profiles with Multiple Fields*, Comput.Phys.Commun. **183** (2012) 2006–2013, [[arXiv:1109.4189](#)].
- [77] A. Arbey, M. Battaglia, A. Djouadi, F. Mahmoudi, and J. Quevillon, *Implications of a 125 GeV Higgs for supersymmetric models*, Phys.Lett. **B708** (2012) 162–169, [[arXiv:1112.3028](#)].
- [78] O. Buchmueller, R. Cavanaugh, M. Citron, A. De Roeck, M. Dolan, et al., *The CMSSM and NUHM1 in Light of 7 TeV LHC,  $B_s$  to  $\mu^+\mu^-$  and XENON100 Data*, Eur.Phys.J. **C72** (2012) 2243, [[arXiv:1207.7315](#)].
- [79] J. R. Ellis and K. A. Olive, *How finely tuned is supersymmetric dark matter?*, Phys.Lett. **B514** (2001) 114–122, [[hep-ph/0105004](#)].
- [80] J. R. Ellis, K. A. Olive, Y. Santoso, and V. C. Spanos, *Supersymmetric Dark Matter in Light of WMAP*, Phys. Lett. **B565** (2003) 176–182, [[hep-ph/0303043](#)].
- [81] J. Ellis and K. A. Olive, *Revisiting the Higgs Mass and Dark Matter in the CMSSM*, Eur.Phys.J. **C72** (2012) 2005, [[arXiv:1202.3262](#)].
- [82] **Planck Collaboration**, P. Ade et al., *Planck 2013 results. I. Overview of products and scientific results*, [arXiv:1303.5062](#).
- [83] G. Belanger, F. Boudjema, A. Pukhov, and A. Semenov, *MicrOMEGAs 2.0: A Program to calculate the relic density of dark matter in a generic model*, Comput.Phys.Commun. **176** (2007) 367–382, [[hep-ph/0607059](#)].
- [84] G. Belanger, F. Boudjema, A. Pukhov, and A. Semenov, *MicrOMEGAs: A Program for calculating the relic density in the MSSM*, Comput.Phys.Commun. **149** (2002) 103–120, [[hep-ph/0112278](#)].
- [85] F. Staub, T. Ohl, W. Porod, and C. Speckner, *A Tool Box for Implementing Supersymmetric Models*, Comput.Phys.Commun. **183** (2012) 2165–2206, [[arXiv:1109.5147](#)].
- [86] **ATLAS Collaboration**, G. Aad et al., *Measurements of Higgs boson production and couplings in diboson final states with the ATLAS detector at the LHC*, Phys.Lett. **B** (2013) [[arXiv:1307.1427](#)].



- [87] G. F. Giudice, P. Paradisi, and A. Strumia, *Correlation between the Higgs Decay Rate to Two Photons and the Muon  $g - 2$* , JHEP **1210** (2012) 186, [[arXiv:1207.6393](#)].
- [88] K. Schmidt-Hoberg and F. Staub, *Enhanced  $h \rightarrow \gamma\gamma$  rate in MSSM singlet extensions*, JHEP **1210** (2012) 195, [[arXiv:1208.1683](#)].
- [89] K. Benakli, M. D. Goodsell, and F. Staub, *Dirac Gauginos and the 125 GeV Higgs*, JHEP **1306** (2013) 073, [[arXiv:1211.0552](#)].
- [90] A. Joglekar, P. Schwaller, and C. E. M. Wagner, *A Supersymmetric Theory of Vector-like Leptons*, [arXiv:1303.2969](#).
- [91] B. Batell, S. Jung, and C. E. M. Wagner, *Very Light Charginos and Higgs Decays*, [arXiv:1309.2297](#).
- [92] M. A. Ajaib, I. Gogoladze, F. Nasir, and Q. Shafi, *Revisiting mGMSB in Light of a 125 GeV Higgs*, Phys.Lett. **B713** (2012) 462–468, [[arXiv:1204.2856](#)].
- [93] H. E. Haber, R. Hempfling, and A. H. Hoang, *Approximating the radiatively corrected Higgs mass in the minimal supersymmetric model*, Z.Phys. **C75** (1997) 539–554, [[hep-ph/9609331](#)].
- [94] M. S. Carena, H. Haber, S. Heinemeyer, W. Hollik, C. Wagner, et al., *Reconciling the two loop diagrammatic and effective field theory computations of the mass of the lightest CP - even Higgs boson in the MSSM*, Nucl.Phys. **B580** (2000) 29–57, [[hep-ph/0001002](#)].
- [95] A. Bartl, T. Gajdosik, E. Lunghi, A. Masiero, W. Porod, et al., *General flavor blind MSSM and CP violation*, Phys.Rev. **D64** (2001) 076009, [[hep-ph/0103324](#)].
- [96] *Search for direct third generation squark pair production in final states with missing transverse momentum and two b-jets in  $\sqrt{s} = 8$  tev pp collisions with the atlas detector.*, Tech. Rep. ATLAS-CONF-2013-053, CERN, Geneva, May, 2013.
- [97] R. Barbieri and G. Giudice, *Upper Bounds on Supersymmetric Particle Masses*, Nucl.Phys. **B306** (1988) 63.
- [98] R. Kitano and Y. Nomura, *Supersymmetry, naturalness, and signatures at the LHC*, Phys.Rev. **D73** (2006) 095004, [[hep-ph/0602096](#)].
- [99] J. R. Ellis, K. A. Olive, and Y. Santoso, *Calculations of neutralino stop coannihilation in the CMSSM*, Astropart.Phys. **18** (2003) 395–432, [[hep-ph/0112113](#)].
- [100] T. Cohen and J. G. Wacker, *Here be Dragons: The Unexplored Continents of the CMSSM*, [arXiv:1305.2914](#).
- [101] J. Harz, B. Herrmann, M. Klasen, K. Kovarik, and Q. L. Boulc’h, *Neutralino-stop co-annihilation into electroweak gauge and Higgs bosons at one loop*, Phys.Rev. **D87** (2013) 054031, [[arXiv:1212.5241](#)].
- [102] H. E. Haber and R. Hempfling, *Can the mass of the lightest Higgs boson of the minimal supersymmetric model be larger than  $m(Z)$ ?*, Phys.Rev.Lett. **66** (1991) 1815–1818.
- [103] M. S. Carena and H. E. Haber, *Higgs boson theory and phenomenology*, Prog.Part.Nucl.Phys. **50** (2003) 63–152, [[hep-ph/0208209](#)].
- [104] A. Djouadi, *The Anatomy of electro-weak symmetry breaking. II. The Higgs bosons in the minimal supersymmetric model*, Phys.Rept. **459** (2008) 1–241, [[hep-ph/0503173](#)].
- [105] M. Frank, T. Hahn, S. Heinemeyer, W. Hollik, H. Rzehak, et al., *The Higgs Boson Masses and Mixings of the Complex MSSM in the Feynman-Diagrammatic Approach*, JHEP **0702** (2007) 047, [[hep-ph/0611326](#)].
- [106] D. M. Pierce, J. A. Bagger, K. T. Matchev, and R.-j. Zhang, *Precision corrections in the minimal supersymmetric standard model*, Nucl. Phys. **B491** (1997) 3–67, [[hep-ph/9606211](#)].

- [107] H. Baer and J. List, *Post LHC7 SUSY benchmark points for ILC physics*, [arXiv:1205.6929](#).